INTERNAL ATMOSPHERIC GRAVITY WAVES IN THE LOWER IONOSPHERE

by

B.G. Fejer

Adviser

D.B.Rai

LAFE-128

August, 1970

SUBMITTED IN PARTIAL FULFILLMENT OF THE REQUIREMENTS FOR THE DEGREE OF MASTER OF SCIENCE

PR - Conselho Nacional de Pesquisas
Comissão Nacional de Atividades Espaciais
São José dos Campos - SP - Brasil

PRESIDÊNCIA DA REPÚBLICA
CONSELHO NACIONAL DE PESQUISAS
COMISSÃO NACIONAL DE ATIVIDADES ESPACIAIS
São José dos Campos - Estado de São Paulo - Brasil

INTERNAL ATMOSPHERIC GRAVITY WAVES IN THE LOWER IONOSPHERE

by

B.G. Fejer

This report contain elements of CNAE's research program and its publication has been approved by

Fernando de Mendonça

Scientific Director

INTERNAL ATMOSPHERIC GRAVITY WAVES IN THE LOWER IONOSPHERE

B.G.Fejer

ABSTRACT

This thesis is concerned with the study of gravity waves in the lower ionosphere using Rocket-Grenade Experiment data. Chapter I presents a general description of the theory of internal gravity waves and the possible sources. Chapter II introduces the data available and the criteria used for the detection of these waves. In Chapter III some atmospheric profiles showing evidence of gravity waves are presented checking the main results predicted by the theory, and the conditions necessary for their occurrence in the lower ionosphere are analyzed. The lack of correlation between magnetic activity and occurrence of waves is significant and so is the seasonal variation evident at all latitudes. The generation of turbulence due to gravity waves is considered briefly in Chapter IV and the main conclusions are presented in Chapter V.

TABLE OF CONTENTS

CHAPTER I

THE THEORY OF INTERNAL GRAVITY WAVES

1.1. Introduction

In recent years considerable interest has developed in the phenomenon of internal atmospheric gravity waves as an important factor related to the dynamical behaviour of the upper atmosphere.

According to Lindzen (1969) gravity waves are those waves whose restoring force comes from the action of gravity in a stratified fluid. In the atmosphere internal gravity waves are due to the atmosphere's continuous potential temperature stratification. The lower limit on the period of these waves is the Brunt-Vaisala period which over most of the earth's upper atmosphere is of the order of 5 minutes. So, gravity waves are to be taken as waves in which the gravitational force plays a dominant role in the determination of the wave properties. They exclude (at least for our purposes) planetary and tidal waves. Their occurrence is irregular and their periods lie usually, in the range 0.1 - 10 hours. Internal atmospheric gravity waves differ somewhat from the gravity waves that form on the surface of the seas and they merge to some extent with acoustic and tidal waves. Their oscillation and propagation are anisotropic due to gravity (Hines, 1965a).

The theory of internal gravity waves was developed by Hines (1960, 1964) and extended by Pitteway and Hines (1963) for an isothermal atmosphere in which the kinematic viscosity or the thermal conductivity (they consider only one at a time) is either constant or of perturbation

magnitude. Press and Harkrider (1962) divided the atmosphere in many isothermal slabs to study the fully ducted modes of atmospheric waves using numerical methods. Friedman (1966), using a similar model, extended the analysis to include partially ducted modes. Midgley and Liemohn (1966) obtained numerical solutions of the linearized equations for gravity waves in a realistic atmosphere including the effects of variable viscosity, thermal conductivity and of temperature gradients. A comprehensive review of the theory of waves in stratified, compressible fluids in a gravity field, at rest with respect to inertial or rotating coordinates and neglecting viscosity and heat conduction, has been given by Tolstoy (1967).

1.2. Internal Gravity Waves in the Upper Atmosphere

Many properties of the irregular winds and waves in the D, E and lower F-regions may be explained by the presence of gravity waves. A full understanding of the effect of these waves will depend in part on an understanding of the propagation conditions and especially of the part played by reflection and ducting.

It has been suggested that although energy flowing upward can be partly reflected below the mesopause or in the lowest part of the thermosphere, an upward leakage of some part of the energy is possible. This energy may be responsible for observed disturbances in the critical frequency of the ionospheric layer, and more especially of the F2-layer. These disturbances are associated with travelling ionospheric disturbances that have been reported by many authors, (Tveten, 1961). The travelling ionospheric

disturbances were initially assumed to be caused as a result of resonant responses of the ionosphere to certain Fourier components of the gravity wave spectrum. Now, these disturbances are more successfully explained attributing them to corresponding disturbances of the neutral gas associated with the passage of internal gravity waves. The horizontal and vertical wavelengths are roughly comparable; they range from 50 to several hundred kilometers in most cases and the periods are typically in the range of 15 - 60 minutes. The TID's(travelling ionospheric disturbances)propagate over very large distances without appreciable attenuation. This led to the suggestion that the wave energy was trapped in a duct extending from ground level to some hypothetical perfectly reflecting region above the level of the TID observation. The difficulty of identifying the necessary upper reflecting region, and the characteristic vertical change of phase in the TID's led Hines (1960) to suggest that the wave energy was strongly reflected at levels somewhat below those of the TID's observations and was strongly ducted between them and the ground, but nevertheless it was subject to some leakage upward into the F-region. Many TID's may be generated by high latitude auroral disturbances in the region between 100 and 150 km. It has been suggested that gravity waves should be radiated from the auroral regions during geomagnetic storms by the following mechanism. Auroral energy deposited as heat in the polar atmosphere causes an expansion of the atmosphere forming a bulge. Some of the potential energy is converted into thermal energy and radiated to low latitudes causing a decay in the polar bulge. During a geomagnetic storm the power input to the neutral gas by Joule heating can increase the scale height by a factor of 5 at altitudes above about 150 km.

Hooke (1968) has studied the effect of internal gravity waves in the production of ionospheric irregularities using a perturbation treatment. He concluded firstly that gravity waves change the ionization rate by changing the local value of the neutral gas density and causing changes in the local value of the ionizing radiation flux due to the variation of absorption undergone by the radiation during its passage. These seem to be important in the daytime gravity wave production of F-region irregularities at the height of the F-1 ledge. Secondly, the rate coefficients of the ion-atom interchange reaction (important in the removal of electrons) are temperature dependent. Lastly, the dominant effect of the gravity waves in the F-2 region is to impart the motion of the neutral gas parallel to the magnetic field lines to the ions through collisional interaction.

According to Hodges (1970), large amplitude fluctuations of winds and gradients of density and temperature, probably due to internal gravity waves, affect the diffusion by non linear processes. Their main effect would be to transport lighter gases downward and heavier gases upward. The common phenomenon of the noticeable decrease of the density scale height in the lower thermosphere can be explained by the application of this result to helium. This effect may disrupt the diffusive equilibrium in the lower F-region causing a mixing of the chemical compositions by briging down the atomic ions (O+) to the region where molecular ions (O_2^+, N_2^+) are dominant.

Hodges (1967, 1969) has suggested that internal gravity waves

can attain turbulence-producing amplitudes and therefore can be a possible source of sporadic turbulence in the upper atmosphere. Turbulence generated by gravity waves in the stratosphere and propagating to the E-region is one possible interpretation of the coupling between stratosphere and ionosphere. This would come about through the change of the chemical composition by affecting the vertical diffusion and hence of some ionospheric parameters such as collision frequency. We shall consider the generation of turbulence due to gravity waves in Chapter IV.

Gravity waves depositing their energy at higher altitudes may be responsible for a significant part of the temperature rise that is observed to occur in the lower E-region during winter. Presently this heating is estimated to be less than the solar input by a factor of 3 to 10 on an average over a day at least at middle latitudes. The small fluctuations superimposed on the general increase in the winter temperature profile are also almost certainly due to gravity waves.

Internal gravity waves may produce magnetic variations propagating through regions of high Hall conductivity (105 - 125 km) although their effect is not so strong as those due to tides and prevailing winds. Also, reports of abnormal meteorological behaviour, at magnetically active times suggest that the gravity waves of wide spectrum, occasionally emitted by jet streams in the stratosphere, may cause a general enhancement in magnetic activity (Hines, 1968) even without a corresponding increase in solar activity.

1.3. Nomenclature and symbols

Some of the important symbols used are listed below:

$x,y,z,$	Cartesian coordinates, with z measured upwards
f	frequency
t	time
m	mass
$\omega = 2\pi f$	angular frequency
ρ	atmospheric density
p	atmospheric pressure
T	atmospheric temperature
Q	heat input due to radiation
$\vec{V}$	fluid velocity
$\vec{\Omega}$	angular velocity of the earth
$\vec{g}$	local gravitational acceleration
$\vec{G}$	gravitational acceleration due to remote bodies
γ	ratio of specific heats
μ	molecular viscosity coefficient
σ_θ	thermal conductivity
k'	Boltzmann's constant
$\vec{E}$	electric field vector
$\vec{B}$	magnetic field vector
$\vec{J}$	electric current density
$i = \sqrt{-1}$	imaginary unit
k	wave number
$c = \sqrt{\frac{\gamma p}{\rho}}$	speed of sound

λ wavelength

τ wave period

$H = \frac{c^2}{\gamma g}$ atmospheric scale height

$\frac{D}{Dt} = \frac{\partial}{\partial t} + \vec{v}.\nabla$ substantive derivative

1.4. Mathematical development

In this section we derive the equations governing the propagation of internal gravity waves. This will be done for the isothermal case, discussed by Hines (1960), because a simple analytic solution is available in this case. After that we shall present a more general solution derived by Midgley and Liemohn (1965) and others.

The basic fluid dynamics equations are:

equation of continuity:

$$\frac{\partial \rho}{\partial t} + \nabla \cdot (\rho \vec{v}) = 0 \qquad (1.1)$$

equation of motion:

$$\rho \frac{\vec{DV}}{Dt} = - \nabla p + \nabla . \vec{\vec{S}} + \rho \vec{g} + \rho \vec{G} - 2\rho \vec{\Omega} \times \vec{V} + \vec{J} \times \vec{B} \qquad (1.2)$$

where the stress tensor $\vec{\vec{S}}$ has components:

$$(\vec{\vec{S}})_{ij} = \mu \left(\frac{\partial V_i}{\partial x_j} + \frac{\partial V_j}{\partial x_i} - \frac{2}{3} \delta_{ij} \nabla . \vec{V} \right)$$

and

∇p - is the force due to pressure,

$\rho\vec{g}$ - the force due to gravity,

$\rho\vec{G}$ - the gravitational force due to remote bodies,

$2\rho\vec{\Omega} \times \vec{V}$ - the Coriolis force,

$\vec{J} \times \vec{B}$ - the Lorentz's force

energy transfer:

$$\frac{\rho k'}{(\gamma-1)m}\frac{DT}{Dt} = Q + \nabla(\sigma_\theta \nabla T) - p\nabla.\vec{V} + \vec{\vec{S}}:\nabla.\vec{V} + (\vec{E} + \vec{V} \times \vec{B}).\vec{J} \qquad (1.3)$$

where

$\frac{\rho k'}{(\gamma-1)m}\frac{DT}{Dt}$ represents the rate of change of internal energy,

$\nabla(\sigma_\theta \nabla T)$ is the heat input due to conduction,

$-p\nabla.\vec{V}$ the flux of energy due to pressure,

$\vec{\vec{S}}:\nabla.\vec{V}$ represents the rate of viscous dissipation of the energy of motion,

$(\vec{E} + \vec{V} \times \vec{B}).\vec{J}$ represents the conversion of electromagnetic energy into thermal energy.

equation of state:

$$p = \frac{\rho k' T}{m} \qquad (1.4)$$

1.4.1. Isothermal case

The isothermal case can be derived making the following assumptions:

1. The curve of the earth is negligible. This assumption is justified for distances from the source smaller than the earth's radius.

2. The rotation of the earth is negligible. This is justified for waves of periods of a few hours or less.

3. The atmosphere is initially isothermal and processes are adiabatic. On the average the atmosphere is adiabatic up to about 100 km; the effect of temperature variation with height will be disucssed in Section 1.4.2.

4. All perturbations vary harmonically in time and in the x and z directions, they have no variations in the y direction.

5. Viscosity is negligible. This will be considered in Section 1.6.2.

6. There are no steady atmospheric winds. The effect of background winds will be discussed in Section 1.6.3.

7. Electric currents in the atmosphere may be ignored. The influence of electric currents will be discussed in Section 1.5.1. and 1.7.

8. The oscillations are sufficiently small so that the equations can be linearized.

Using these assumptions eqs(1.1),(1.2),(1.3), and (1.4) can be written as

$$\frac{\partial \rho}{\partial t} + \nabla(\rho V) = 0 \tag{1.5}$$

$$\rho \frac{D\vec{V}}{Dt} = - \nabla p + \rho \vec{g} \tag{1.6}$$

$$\frac{\rho k'}{(\gamma-1)m} \frac{DT}{Dt} = - p \nabla . \vec{V} \tag{1.7}$$

$$p = \frac{\rho k'}{m} T \tag{1.8}$$

Using (1.8), (1.7), and (1.5), after some transformations we get:

$$\frac{Dp}{Dt} = \frac{\gamma p}{\rho} \frac{D\rho}{Dt} \tag{1.9}$$

or

$$\frac{Dp}{Dt} = c^2 \frac{D\rho}{Dt} \tag{1.10}$$

Defining the background state by ρ_o, p_o, T_o ($\vec{V}_o = 0$) and the perturbations by

$$\rho', p', T', \vec{V}'$$

in the perturbed state we have

$$\rho = \rho_o + \rho'$$
$$p = p_o + p'$$
$$T = T_o + T'$$
$$\vec{V} = \vec{V}'$$

Using these relations in (1.5), (1.6), (1.8), and (1.10) we obtain the zero-order equations:

$$- \nabla p_o + \rho_o \vec{g} = 0 \tag{1.11}$$

$$\rho_o = \frac{p_o}{RT_o} \tag{1.12}$$

Substituting for ρ_o in (1.11) and integrating from ground to a height z, we get

$$p_o = p_g \exp(-z/H) \tag{1.13}$$

and also

$$\rho_o = \rho_g \exp(-z/H) \tag{1.14}$$

where p_g and ρ_g are the ground level values of pressure and density respectively.

The first order equations are

$$\frac{\partial}{\partial t} \rho' + (\vec{V}'.\nabla)\, \rho_o + \rho_o\, \nabla.\vec{V}' = 0 \tag{1.15}$$

$$\rho_o \frac{\partial \vec{V}'}{\partial t} + \nabla p' - \rho' \vec{g} = 0 \tag{1.16}$$

$$\{\frac{\partial \rho'}{\partial t} + (\vec{V}'.\nabla) p_o\} - C^2 \{\frac{\partial \rho'}{\partial t} + (\vec{V}'\nabla)\, \rho_o\} = 0 \tag{1.17}$$

Substituting the values of ρ_o and p_o from (1.13) and (1.14) into (1.15), (1.16), and (1.17) we get

$$\frac{\partial \rho'}{\partial t} - V'_z \cdot \frac{\rho_o}{H} + \rho_o \nabla.\vec{V}' = 0 \tag{1.18}$$

$$\rho_o \frac{\partial \vec{V}'}{\partial t} + \nabla p' - \rho' \vec{g} = 0 \tag{1.19}$$

$$\{\frac{\partial \rho'}{\partial t} - V'_z \frac{p_o}{H}\} - C^2 \{\frac{\partial \rho'}{\partial t} - V'_z \frac{\rho_o}{H}\} = 0 \tag{1.20}$$

As stated before, we are considering only the two dimensional case in which $\partial/\partial y = 0$. Wave solutions of the set (1.18)-(1.20) may be found in a complex Fourier form such that p'/p, ρ'/ρ, V'_x and V'_z all have the same exponential form proportional to

$$\Phi \equiv \exp\left(\frac{z}{2H}\right) \exp\{i(\omega t - k_x x - k_z z)\} \tag{1.21}$$

so that

$$\frac{p'}{Pp_o} = \frac{\rho'}{R\rho_o} = \frac{V'_x}{X} = \frac{V'_z}{Z} = A \exp\left(\frac{z}{2H}\right)\exp\{i(\omega t - k_x x - k_z z)\} \tag{1.22}$$

where A is a constant and P, R, X and Z are relative amplitudes to be determined. The first exponential in (1.21) describes an amplitude growth of the perturbations (provided that it is not offset by an imaginary component of k_z) and, in practice, this helps to account for the importance of the waves at ionospheric heights. This property is a consequence of the conservation of kinetic energy $\rho_o A^2(|X|^2 + |Z|^2)$ with height since the density falls off as $\exp(-z/H)$.

Using relations (1.22) in (1.18), (1.19) and (1.20) and separating the equation resulting from (1.19) into its two components we get

$$\begin{aligned}
&(i\omega)R + (-ik_x)X + (-\frac{1}{2H} - ik_z)Z + (0)P = 0\\
&(0)R + (i\omega)X + (0)Z + (-ik_x)\frac{p_o}{\rho_o}P = 0\\
&(g)R + (0)X + (i\omega)Z + (-\frac{1}{2H} - ik_z)\frac{p_o}{\rho_o}P = 0\\
&(-i\omega)R + (0)X + (\frac{1}{H} - \frac{p_o}{\rho_o HC^2})Z + (i\omega)\frac{p_o}{\rho_o}P = 0
\end{aligned} \qquad (1.23)$$

This homogeneous system of equations has a solution if and only if the determinant of its coefficients vanishes, i.e.

$$\begin{vmatrix}
i\omega & -ik_x & -\frac{1}{2H} - ik_z & 0\\
0 & i\omega & 0 & -ik_x\\
g & 0 & i\omega & -\frac{1}{2H} - ik_z\\
-i\omega & 0 & \frac{1}{H} - \frac{p_o}{\rho_o HC^2} & i\omega
\end{vmatrix} = 0$$

Resolving this determinant we get

$$\frac{\omega^4}{C^2} - \omega^2(K^2_x + k^2_z) + g\frac{k^2_x}{H}(1 - \frac{p_o}{\rho_o C^2}) - \frac{\omega^2}{4H^2} = 0 \qquad (1.24)$$

or

$$\omega^4 - \omega^2C^2(k^2_x + k^2_z) + (\gamma - 1)g^2k^2_x - \frac{\gamma^2g^2}{4C^2}\omega^2 = 0 \qquad (1.25)$$

This is the dispersion equation derived by Hines (1960).

The values of the relative amplitudes can be obtained by solving the system (1.23).

$$P = \gamma\omega^2 \left| k_z - i\left(1 - \frac{\gamma}{2}\right) \frac{g}{2C^2} \right| \tag{1.26}$$

$$R = \omega^2 k_z + i(\gamma - 1)\, g k_x^2 - i\, \frac{\gamma g \omega^2}{2C^2} \tag{1.27}$$

$$X = \omega k_x^2 C^2 \left| k_z - i\left(1 - \frac{\gamma}{2}\right) \frac{g}{C^2} \right| \tag{1.28}$$

$$Z = \omega(\omega^2 - k_x^2 C^2) \tag{1.29}$$

From eqn. (1.25) we have

$$\omega^4 - \omega^2 C^2 (k_x^2 + k_z^2) + C^2 \omega_g^2 k_x^2 - \omega_a^2 \omega^2 = 0 \tag{1.30}$$

where

$$\omega_g \equiv \frac{(\gamma - 1)^{\frac{1}{2}}\, g}{C}$$

and

$$\omega_a \equiv \frac{\gamma g}{2C} \quad (\omega_a > \omega_g \text{ because } \gamma < 2 \text{ in the atmosphere})$$

Calculating k_z^2 from (1.30) we get:

$$k_z^2 = \left(\frac{\omega_g^2}{\omega^2} - 1\right) k_x^2 + \frac{(\omega^2 - \omega_a^2)}{C^2} \tag{1.31}$$

In this equation ω_a is the highest possible frequency of oscillation of the atmosphere as a whole; ω_g is the natural frequency of

local oscillations and thus it is just the Brunt-Vaisala frequency for the isothermal case. In the mesosphere the periods corresponding to ω_a and ω_g are about 4.4 min. and 4.9 min. respectively.

The anisotropy caused by gravity is already evident in the dispersion equation (1.30) since k_x and k_z enter into that equation differently except when $g = \omega_g = 0$. When k_x is real it is evident from eqn.(1.31) that k_z may be purely real or purely imaginary. In the first case the waves will be internal, in the other case they will be evanescent waves. These evanescent waves have been referred to in the past as surface waves because of the lack of their phase progression; but the term evanescent is preferable because these acoustic-gravity waves exist independently of any surface.

An examination of (1.30) shows that in the case of internal waves, the frequency range $\omega_g < \omega < \omega_a$ is forbidden, so that the available spectrum gets divided into two different regions. The frequency range $\omega > \omega_a$ is termed acoustic range because in the high frequency limit the dispersion equation (1.30) becomes

$$(k^2_z + k^2_x) = \frac{2}{c^2}$$

which corresponds to ordinary sound waves; the low frequency range characterized by $\omega < \omega_g$ is termed internal gravity wave range. For many applications, that require the consideration of evanescent waves and waves with complex k_x, the two categories mentioned above are considered as divisions of a broader class termed acoustic-gravity waves.

The two sequences may be distinguished clearly using the normalized coordinates:

$$n_x = \frac{k_x C}{\omega} \qquad \text{and} \qquad n_z = \frac{k_z C}{\omega} \tag{1.32}$$

which correspond to components of a refractive index vector.

Introducing n_x and n_z in the dispersion equation (1.30) we get

$$\omega^2 |1 - (n^2_x + n^2_z)| + \omega g^2 n^2_x - \omega^2_a = 0 \tag{1.33}$$

or

$$n^2_z = (1 - \frac{\omega^2_a}{\omega^2}) - n^2_x (1 - \frac{\omega^2_g}{\omega^2}) \tag{1.34}$$

Figure 1 shows (1.34) as function of n_x and n_z for various values of the wave period.

For the outermost ellipse we have $\omega >> \omega_a$ (and also $\omega >> \omega_g$) so that (1.33) reduces to

$$n^2_x + n^2_z = 1$$

which corresponds to the equation of a circle representing waves that propagate with the speed of sound. The contours inside this circle obviously have $n < 1$ and they represent waves that travel faster than the sound. On the other hand the contours outside the circle have $n > 1$ so that

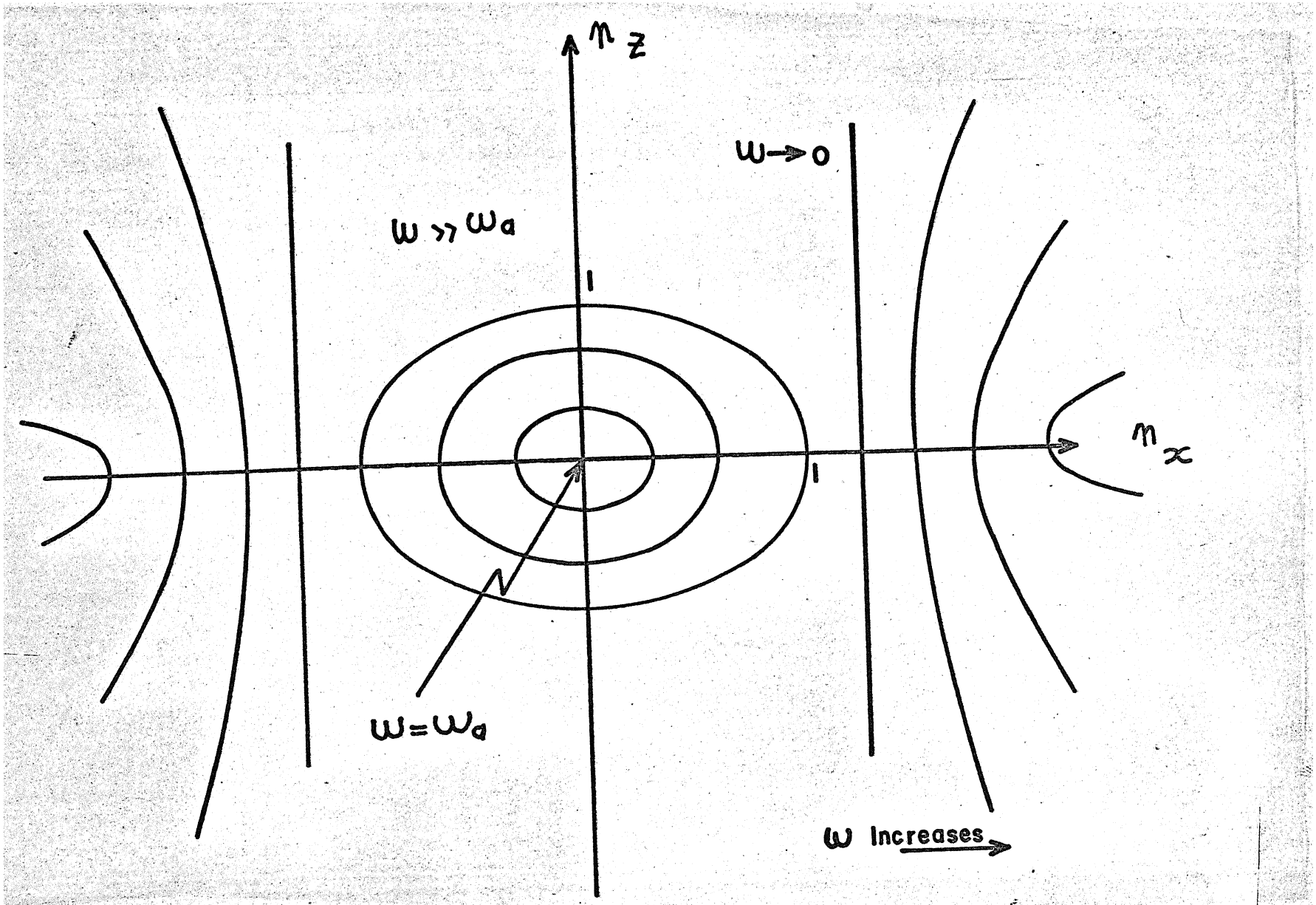

Fig. 1 - Dispersion curves for atmospheric waves in terms of the refractive indices

they propagate with speed smaller than that of sound. It may also be seen that acoustic waves with periods close to ω_a propagate faster than their high frequency conterparts, whereas internal gravity waves, in general, propagate more slowly.

1.4.2. Realistic atmosphere

Here we present the dispersion equation for a more realistic atmosphere taking into account thermal gradients and dissipation. Still the following hypotheses must be used:

1. The curvature of the earth is negligible.
2. There are no steady atmospheric winds.
3. The rotation of the earth is negligible.
4. All perturbations vary harmonically in time in the x and z directions. They have no y derivative.

The major approximation is the linearization of the basic equations. This has to be done because exact solutions are very difficult. Considering the hypotheses stated above the fundamental eqs.(1.1), (1.2), (1.3), and (1.4) can be written as

$$\begin{aligned}
&\frac{\partial \rho}{\partial t} + \nabla.(\rho\vec{V}) = 0 \\
&\rho \frac{D\vec{V}}{Dt} = \rho\vec{g} - \nabla p + \nabla.\vec{\vec{S}} \\
&\frac{\rho k'}{(\gamma - 1)m} \frac{DT}{Dt} = Q + \nabla.(\sigma_\theta \nabla T) - p\nabla.\vec{v} + \vec{\vec{S}} :\nabla.\vec{v} \\
&p = \frac{\rho k' T}{m}
\end{aligned} \tag{1.35}$$

The solutions of this sytem for gravity waves must be obtained numerically because the amplitudes of the perturbations are functions of altitude. To do this the atmosphere is divided into thin layers, and in each layer the atmospheric parameters are assumed constant so that analytic solutions may be obtained. In doing this Midgley and Liemohn (1966) used a model in which μ and σ_θ vary as exp(-z/H) whithin a given layer above about 120 km; at lower altitudes the molecular viscosity blended with a suitable model for eddy viscosity. They obtained the following dispersion equation in each layer

$$C_3R^3 + C_2R^2 + c_1R^1 + C_o = 0 \tag{1.36}$$

where

$$R = - \left| 1 + \left(\frac{k_z}{k_x}\right)^2 \right| + i\alpha \frac{k_z}{k_x}$$

$$C_0 = \frac{1}{\gamma - 1} \left| \beta^2 - 2\eta\alpha^2 (1 + 3\eta) \right| + \alpha^2(3\eta + 1)$$

$$C_1 = \nu\left|\beta^2 - 2\eta\alpha^2(1 + 3\eta)\right| + \frac{\beta}{\gamma - 1} (1 + 7\eta) + \beta \tag{1.37}$$

$$C_2 = \frac{3\eta}{\gamma - 1} (1 + 4\eta) + \beta\nu(1 + 7\eta) + 3\eta$$

$$C_3 = 3\eta\nu(1 + 4\eta)$$

$$\nu = \frac{i\sigma_\theta k_x^2}{\omega\, p_o}$$

$$\beta = \frac{\omega^2}{gHk_x^2}$$

$$\eta = \frac{i\omega\mu}{3p_o}$$

$$\alpha = \frac{1}{Hk_x}$$

Since (1.36) is a sixth-order equation there are four other solutions in addition to the upgoing and downcoming gravity waves. Two of these solutions correspond to viscous waves resulting from the interaction of viscous and inertial forces. The other two correspond to thermal waves resulting from the effects of heat capacity and heat conductivity. Although all four of these waves damp rapidly, especially in the lower atmosphere, their presence prevents the solution of eqn.(1.36) by conventional numerical methods (Midgley and Liemohn, 1966).

1.5. Sources of Gravity Waves in the Atmosphere

One of the most important problems in the evaluation of the role of internal gravity waves is the identification of sources with a good degree of certainty. In spite of the fact that there are many possible sources only auroral-zone currents and, on one occasion, a major earthquake (Alaskan earthquake in 1964) have been identified with some degree of certainty. Although some isolated localizations have been made since 1960, methods for reliable identification of sources are still needed. The identification difficulty comes in part from the breadth of the observed spectra and even more so from the breadth of the spectra emitted. This difficulty is increased by the filtering action of the intervening levels especially those associated with regions where the waves are evanescent. The difficulties also stem from the techniques used until now for the identification of sources. Thus the ray tracing technique, that can be used for calculating the energy flux, or the

method considering the propagation of a wave packet, is not satisfactory under some conditions of the upper atmosphere. This occurs due to imperfectly known wind systems of the middle atmosphere especially in regions of evanescence. The ray tracing is a good approximation when most of the energy is reflected (unless one's concern is with the small portion that gets through); when this does not occur, then another method must be used for following the energy after it reaches the reflection level ($K_z = 0$). In the following section we shall describe the possible sources of gravity waves in the atmosphere, mostly in the lower atmosphere; we shall discuss in some detail the role played by the mechanisms in the auroral zone and in the equatorial zone.

1.5.1. Possible sources

Among the possible sources we can quote the following:

1. Sources in the auroral and equatorial zones. Many observations in recent years have demonstrated that auroral activity or some mechanism related with it can produce waves in the atmosphere. Wilson and Nichparenko (1967) detected infrasonic waves at the ground by sensing pressure variations associated with auroral activity. Hunsucker and Tveten (1967) associated internal gravity waves at ionospheric F-region heights with auroral events. The observations suggest that all possible modes from pure acoustic to internal gravity waves are possible under appropriate conditions.

Several authors have demonstrated theoretically that intense energy input into the auroral thermosphere during a magnetic substorm could

generate gravity waves compatible with the observations (Hines, 1965). Experimentally the equatorward directions of these waves and their relation to magnetic activity suggests an auroral origin. In the case of TID's the equatorward propagation from auroral zones has been reported by many workers using various techniques (Hunsucker and Tveten, 1967). Among these we have simultaneous observations from ground networks of rapid sequence ionosondes and topside sounding from satellites, irregularities in the Faraday rotation and study of large travelling disturbances in the ionosphere using incoherent scatter technique. The exact mechanism responsible for the transmission of the energy, however, is not known precisely. Charzanowski et. al.(1961) have suggested the possibility of trapping of the energy in the E-layer and so ground measurements would be a consequence of the leakage from the bottom of the duct. Thome (1968) has suggested that the wave trains observed at Arecibo, Puerto Rico,represented energy propagated in fully and partially ducted modes along the base of the thermosphere.

There are several mechanisms proposed for the generation of the wave motion. The waves observed by Tveten (1961) were probably generated by an impulsive mechanism when a sudden influx of energetic particles caused intensive heating in the auroral latitudes. Maeda and Watanabe (1964) postulated that regions of pulsating auroras give rise to infrasonic waves. The energy sources for this type of auroral activity are not necessarily incident auroral particles, but a flow of secondary electric currents called the auroral electrojet. Although there is no experimental evidence of the action of the equatorial electrojet in the generation of these waves, it must play a similar role, at least theoretically, as the auroral electrojet.

The two main processes by which auroral and equatorial currents may generate gravity waves are:

a. Joule coupling, heating of the neutral air due to the Joule effect. The Joule heating is given by J^2/σ_3, where σ_3 is the Cowling conductivity. Significant differences of efficiency may result from differences of the Cowling conductivity. Testud and Vasseur (1970) studied the effect of Joule heating in the generation of gravity waves observed at middle latitudes. They used a heat source function characterized by a latitudinal width, a vertical thickness, a maximum heat production altitude and the time duration of the storms. The latitudinal width is about 6^o for both electrojets, the vertical widths are about 60 km, the altitude of maximum heat production about 150 km. The periods of auroral magnetic variations are about 15 to 60 min.; for the equatorial electrojet periods of 40 to 50 min. are quite common. The current density of the auroral electrojet varies from about 3×10^{-5} to 10^{-4} A/cm^2; in the equatorial electrojet it is smaller by a factor of perhaps one-third. Cole (1962 a,b) estimates that during a moderate geomagnetic storm the power input to the neutral gas in the auroral region by Joule heating is about 4×10^{10} W. A part of this energy can be radiated to lower latitudes.

b. The Lorentz's force ($\vec{J} \times \vec{B}$), set up by the electric currents of the auroral and equatorial electrojets and transferred from the ionized components to the neutrals via collisions (Lorentz coupling). Since for both electrojets the length is large compared with their width, they will act as line sources at ranges comparable or less than their respective lengths. The significant difference is the direction of the driving force, so the nature of the Lorentz coupling is quite different in the two regions. In the auroral regions the geomagnetic field is almost vertical and the coupling proceeds through a transfer of horizontal momentum to the neutral gas. At the equator the geomagnetic field is almost horizontal and the Lorentz force is vertical. This fact would certainly influence the nature of the waves generated and probably the radiated energy. Chimonas (1970) coucluded that the Lorentz coupling is very much weaker in the equatorial region. But he also concluded that even in the equatorial region the Lorentz coupling is more effective than the Joule coupling in the generation of TID's. In the auroral region it is not known which mechanism is dominant (Chimonas and Hines, 1970a). Knudsen (1969) estimated that the amplitude of the waves generated at the equator are about one-tenth of those generated in the auroral zone and, hence, is below the lower limit of detectability with the present detection techniques (Thome, 1968).

2. Surface waves over mountains and ridges. In the case of steady winds we have a standing wave field as shown in Fig.2. If the velocity is variable we have propagating waves. The hills of Wales, for example, are reported to give rise to relatively narrow spectrum of waves under appropriate wind conditions. Variable winds across the Rocky Mountains should yield a broad spectrum of waves, with waves of differing periods launched at different angles of elevation. In this case the characteristic variation of the wave period would be produced at any given level in the atmosphere, while the azimuthal spreading must be minimized by the great length of the mountain system.

3. Nonlinearities in tidal waves. Sometimes, the tidal waves can attain such large amplitude variations that nonlinear effects become very important. In these cases waves may be generated, some of which may be gravity waves.

4. Weather fronts can form bulges in the troposphere that might be responsible for the generation of gravity waves that are observed at higher altitudes. Gossard (1962) observed the effect of gravity waves in pressure and wind measurements in Southern California. He also suggested the possibility of the occurrence of a window for periods of about 10 minutes to 2 hours through which fairly large amounts of energy sometimes flow out of the troposphere.

5. Wind shears associated with turbulence are another possible source of gravity waves because of the motion of the gas that they can generate. In particular, wind shears associated with jet streams (that is two very strong wind shears) should be important.

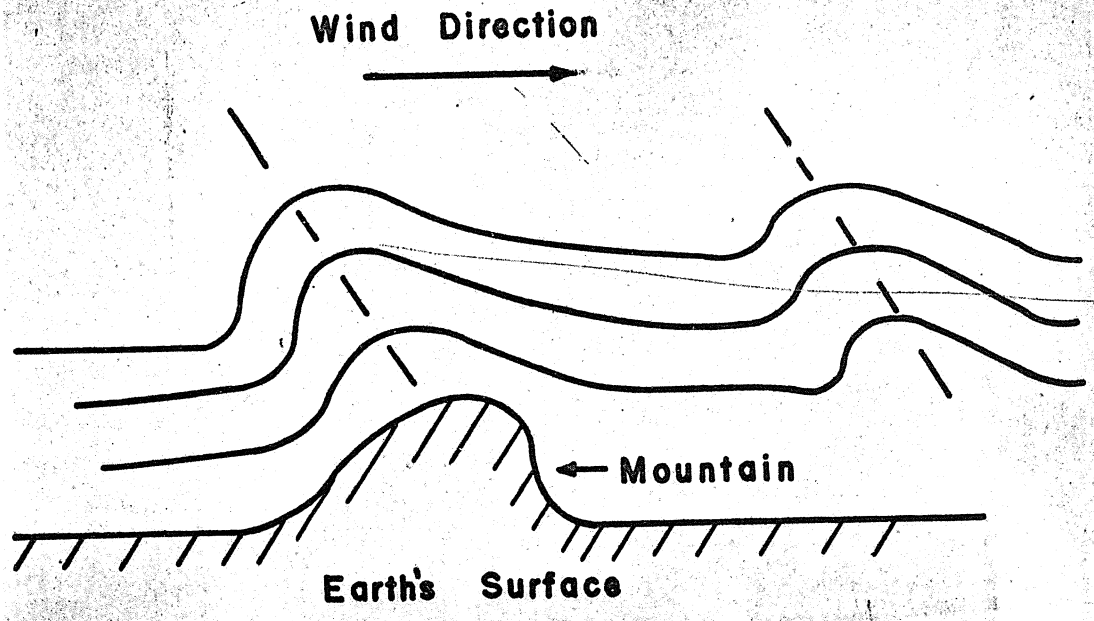

Fig. 2 - Generation of waves due to winds flowing over mountains

6. Nuclear explosions are sources of waves that have attracted the attention of many workers (Row, 1967; Hines, 1967). Large nuclear detonations cause long period oscillations that have been interpreted in terms of long period gravity waves. Their effects can be observed in the variations of the F-layer critical frequency even far from the explosion site. When a nuclear explosion occurs a "fire-ball" is formed which expands at a very high velocity. As a consequence a shock wave is generated which propagates away from the source. This shock wave loses its energy rapidly and degenerates into a linear pressure waves. Lomax and Nielson (1968) postulated that the pressure wave evolves into an acoustic-gravity wave; the particular excited mode may depend upon the energy distribution of the pressure wave as a function of altitude and horizontal position. They also suggested that away from the source (beyond 1000 km) the propagation of the wave may be maintained by the neutral component of the atmosphere. An interesting feature, seen in the ionograms during nuclear explosions, is the nearly linear increase of the period of oscillation with increase in range of the observer from the source. This increase, which is predicted by the theory of pulse propagation in a plane isothermal neutral atmosphere, can be explained by dispersion of the wave packet.

7. Earthquakes are other sources of gravity waves that have been studied extensively. The long period disturbances caused by the Alaskan earthquake of 1964 were seen in great detail in ionograms and Doppler records. Row (1967) has suggested that these perturbations (period approximately 90 minutes) may be an acoustic-gravity wave pulse launched by the major ground displacement near the epicenter.

8. Solar eclipse may induce atmospheric gravity waves. This may happen because during a solar eclipse there is an interference with the heat balance in the shadowed portion of the atmosphere which can generate gravity waves. Chimonas and Hines (1970 b) have found that at points whose perpendicular distance from the path of the eclipse is 10 000 km the expected maximum pressure perturbation is sufficient to permit detection by microbarographs as travelling ionospheric disturbances.

1.6. Propagation of Internal Gravity Waves

Now we deduce the conditions of propagation of internal gravity waves, initially for the simple isothermal case with no background winds. Later on we shall investigate the effect of the background wind and present the results obtained by the use of more realistic approaches.

1.6.1. Propagation of gravity waves in an isothermal atmosphere

The wave packet concept is useful for investigating the propagation of energy carried by acoustic-gravity waves. The wave packet method considers a superposition of plane waves having different frequencies and directions of propagation. The regions of maximum amplitude are associated with concentrations of energy. Although the correspondence between the propagation of wave packets and energy flow is not always complete it is good enough for many purposes. It can be shown easily that the velocity of energy propagation is given by the vector components

$$\frac{\partial \omega}{\partial k_x}, \frac{\partial \omega}{\partial k_y}, \frac{\partial \omega}{\partial k_z} \qquad (1.38)$$

The form of eqn.(1.36) contains a useful result for it shows that the energy velocity is just the gradient of $\omega(\vec{k})$ in a $\vec{k}$ space.

Let us return to the dispersion equation(1.30) which is rewritten below for convenience

$$\omega^4 - \omega^2 c^2 (k_x^2 + k_z^2) + c^2 \omega_g^2 k_x^2 - \omega_a^2 \omega^2 = 0 \qquad (1.30)$$

The general behaviour of this dispersion relation for pure acoustic and internal gravity waves is shown in Fig.3. The two familes can be clearly distinguished; the family of ellipses represents a sequence of acoustic waves, while the superimposed family of hyperbolas represents a sequence of internal gravity waves. We can immediately find some differences between acoustic and gravity waves. For acoustic waves the wavelength is practically fixed once the period is specified. This is not so for gravity waves, because a whole range of wavelengths is allowed for a given period. For acoustic waves if k_x is fixed, k_z increases with ω while for gravity waves it is the opposite. But the most significant differences are in the direction of energy propagation. From Fig.2. we can see that for acoustic waves the energy propagates in much the same direction as does the corresponding phase pattern, although there is some tendency towards a more vertical flow. On the other hand, for gravity waves the energy may propagate in directions which may differ from the direction of propagation of the phase pattern by as much as 90^o in the asymptotic cases. It should also be noticed that for internal gravity waves the vertical component of energy flow is opposite in sense to the vertical component of phase progression.

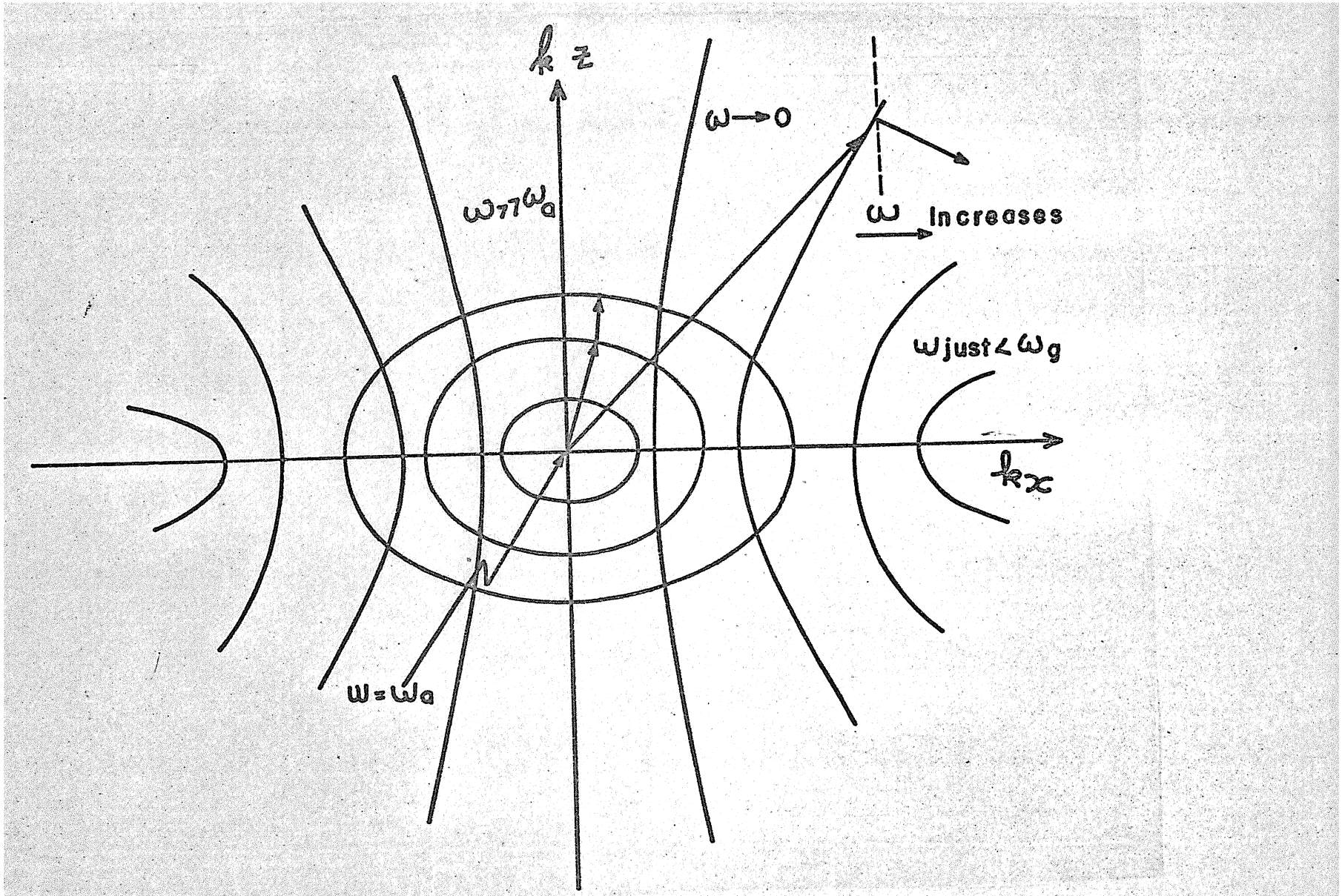

Fig. 3 - Dispersion curves for atmospheric waves in terms of the wave numbers

After some transformations eqn.(1.30) can be written as

$$\left(\frac{k_z}{k_x}\right)^2 = \frac{\omega_g^2 - \omega^2}{\omega^2} + \frac{\omega^2 - \omega_a^2}{k_x^2 C^2} \tag{1.39}$$

If the second term on the left is small in comparison with the two others, eqn.(1.39) becomes

$$\left(\frac{k_z}{k_x}\right)^2 \simeq \frac{\omega_g - \omega^2}{\omega^2} \tag{1.40}$$

or

$$\frac{k}{k_x} \simeq \pm \frac{\omega_g}{\omega} \tag{1.41}$$

for gravity waves this approximation is valid for $k_z >> 1/2$ H. When this is true the hyperbolas of constant ω nearly coincide with their straight line asymptotes. From Fig.4. we can see that eqn.(1.41) represents the maximum angle of phase propagation for a given period. so that

$$\lim \alpha_{phase} = \cos^{-1} \frac{k_x}{k} = \cos^{-1} \frac{\omega}{\omega_g} \tag{1.42}$$

From Fig.3 we note that for acoustic waves the angle of phase propagation α may have any direction while for gravity waves it is restricted to values within the limits $\pm \lim \alpha_{phase}$. The limiting angle for the propagation of energy can be easily shown to be

$$\lim \alpha_{group} = \sin^{-1} \frac{\omega}{\omega_g} \tag{1.43}$$

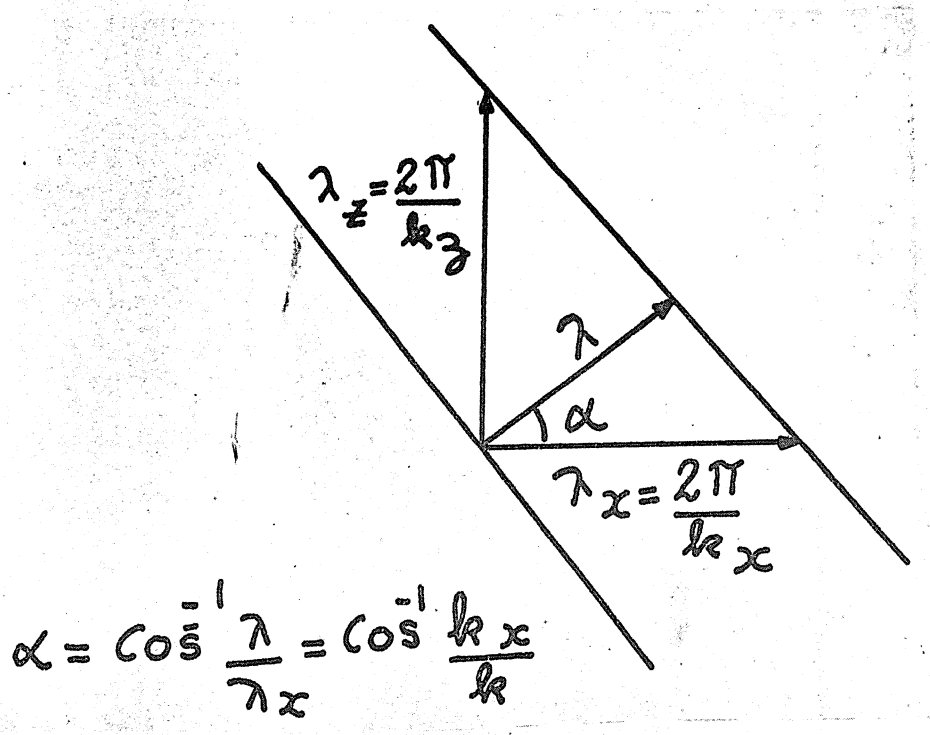

$$\alpha = \cos^{-1}\frac{\lambda}{\lambda_x} = \cos^{-1}\frac{k_x}{k}$$

Fig.4 - Determination of the angle of propagation

1.6.2. Effects of temperature variation

When one considers temperature variation the study of the propagation of gravity waves becomes much more difficult. In this case it is necessary to use more sophisticated methods such as phase integral solutions and WKB solution (Hines, 1965, 1968). For evanescent wave regions the concept of wave packet velocity is not valid and so it is necessary to use other means to obtain the energy flux. An useful way is to use the conventional definition of energy flux averaged over one cycle.

In the case of the earth's atmosphere it is a common practice to use the following procedure used by Press and Harkrider (1962). The atmosphere is stratified into isothermal layers, and for each layer the linearized nondissipative fluid mechanical equations are solved subject to certain boundary conditions at the interfaces. Strong reflections in a thermally stratified atmosphere may result in the formation of ducts. In some cases total reflection occurs and the energy of the wave propagates horizontally in the duct without loss (perfect ducting). In other cases, however, the reflection is not total but is nevertheless strong, thus the wave energy, is carried to great distances with only small losses in the form of leakage into the overlying regions (imperfect ducting). Friedman (1966) studied imperfect ducting using a full wave treatment and thermally stratified atmospheres representative of summer and winter conditions. He concluded that strong ducting can occur in the troposphere, mesosphere and E-region. Thome (1968) used a two layer atmosphere unbounded above and below. This eliminates partially ducted modes that depend upon ground

reflections. Thus one has only boundary waves propagating at the interface and evanescent waves above and below it. He calculated a phase speed which is in good agreement with travelling ionospheric disturbances observed at Arecibo, Puerto Rico.

1.6.3. Effects of background winds

The occurrence of background winds can affect appreciably the propagation of gravity waves leading to further problems of refraction and reflection. Let ω be the frequency of a wave in a stationary coordinate system, the frequency $\bar{\omega}$ of the same wave in a coordinate system moving with velocity $\vec{v}_o$ of the wind will be

$$\bar{\omega} = \omega - \vec{k}.\vec{v}_o$$

This is simply the Doppler effect. The dispersion equation, although not changing in terms of $\bar{\omega}$, does change in terms of ω. It is no longer symmetric in ω due to the cross term involving ω in the expansion of $(\omega - \vec{k}.\vec{v}_o)^2$. As a consequence there will be different behaviors for positive and negative values of ω. It is possible that the same wave has positive and negative frequencies in the inertial and moving systems respectively. The components of the phase velocity will be given by

$$\frac{\omega}{k_j} = \frac{\omega}{k_j} + \frac{(\vec{k}.\vec{v}_o)}{k_j} \qquad (j = x,y,z)$$

and those of the group velocity by

$$\frac{\partial \omega}{\partial k_j} = \frac{\partial \bar{\omega}}{\partial k_j} + v_{oj}$$

For a coordinate system moving with a horizontal background wind with $v_{ox} > \omega/k_x$, gravity waves can have upward energy and phase propagation. If the background wind is not constant, the multilayer technique is to be applied. Each of the layers has its proper frequency but they must be same at the interfaces. As a wave approaches its critical level ($\omega = \vec{k}.\vec{v}_o$), it seems that total dissipation occurs due to viscosity and thermal conductivity. It has been suggested that winds of the mesosphere can act as a directional filter on the gravity wave spectrum (Hines, 1965, 1968). Thus the waves that can penetrate to higher levels carry information about the winds system they have passed through.

1.7. Energy Dissipation

The observed decrease of wave energy with increase of height is due mainly to dissipation although partial reflections, associated with variations of temperature or of background winds, also contribute to this effect. The main reasons of dissipation are visocsity, thermal conductivity and hydromagnetic damping.

Internal gravity waves can be dissipated by different mechanisms characterized by kinematic viscosity and eddy viscosity. Above 120 km the kinematic viscosity is more important but below 110 km the eddy viscosity is dominant. The dissipation characterized by the eddy viscosity is related to turbulence and will be considered in some detail in chapter

IV. Here we consider only the effect of kinematic viscosity. Whenever the energy dissipation per cycle is small compared to the mean energy available, one can make an estimate of its importance from the results of the inviscid treatment (Hines, 1960). The height, where the ratio of the dissipated energy per unit cycle to the perturbation wave energy becomes comparable to unity, can then be taken as an upper limit for the height to which that mode can propagate without appreciable damping. This height is just the upper limit because the losses due to thermal conductivity were neglected. Using this behaviour it can be deduced that for gravity waves ($\omega < \omega_g$) viscosity will be important in regions for which

$$n \gtrsim 0.17 \frac{\omega}{k^2} \qquad \text{for} \qquad k_z^2 >> \frac{1}{4H^2} \tag{1.41}$$

The effect of thermal conductivity can be studied using the previous method. The losses due to thermal conduction are comparable in magnitude to those of viscosity. The dispersion equation resulting from the simultaneous consideration of both effects was given in section 1.4.2. Below 110 km viscosity and thermal conductivity dissipate the energy of shorter-wave modes (wavelength smaller than 10 km) in distances of the order of a wavelength; the longer wave modes are dissipated at greater heights (Hines, 1960; Kochanski, 1964). Hydromagnetic dissipation results from electric currents that are induced in the ionosphere when a gravity wave propagates through it. Gravity waves with periods of about an hour or greater are severely damped by this effect when they reach 130 km. At night the number of ions present is much smaller and so gravity waves are not severely damped. The hydromagnetic dissipation introduces a new anisotropy and selective damping because it depends upon the direction of propagation.

1.8. Comparison Between Atmospheric and Radio Waves

In an isothermal atmosphere there are some intersting similarities between atmospheric waves and radio waves. Analogies can be drawn (Hines, 1965 a; Davies et al, 1969) between VHF waves in the ionosphere and sound waves, and between whistler waves and gravity waves. Gravity waves and whistler waves (very low frequency electromagnetic waves that may propagate through the magnetosphere) are dispersive (frequency dependent) and anisotropic (depending on direction). In the case of whistler waves (or in general radio waves) the anisotropy results from the effect of the geomagnetic field on the electron motion of the air parcels. Indeed the form of the gravity wave curves in Fig.1 is not unlike the corresponding curves for whistlers if the geomagnetic field were taken as the x-axis. With these analogies ω_a and ω_g correspond to ω_N (plasma frequency) and ω_H (gyrofrequency) respectively. Let us use the notations

$$x = \left(\frac{\omega_a}{\omega}\right)^2 \qquad y = \left(\frac{\omega_g}{\omega}\right)$$

for atmospheric waves and

$$x_r = \left(\frac{\omega_N}{\omega}\right)^2 \qquad y_r = \frac{\omega_H}{\omega}$$

for radio waves

where the index r indicates that we are refering to radio waves. The refractive indices for sound waves and VHF radio waves ($y_r << 1$) are given by

$$N^2 \simeq 1 - X \qquad \text{(sound waves)}$$

$$N_r^2 \simeq 1 - X_r \qquad \text{(VHF radio waves)}$$

these are expected values because for $y \ll 1$ both waves are nearly isotropic. For long period gravity waves ($x \gg 1$, $Y \sin \phi \gg 1$ where ϕ is the angle with the vertical) and whistler waves ($x_r \gg 1$. $Y_r \cos \theta$, where θ is the angle with the direction of magnetic field vector).

$$N^2 \simeq \frac{X}{Y^2 \sin^2 \phi} \qquad \text{(gravity waves)}$$

$$N^2 \simeq \frac{X_r}{Y_r \cos r} \qquad \text{(whistler waves)}$$

Davies et al (1969) have shown analogies between some magnetionic ray formulas and corresponding formulas for atmospheric waves in an isothermal atmosphere. There are also some distinctions between gravity waves and whistlers. Gravity waves do not present splitting into differently polarized components, they are not gyrotropic, and in the absence of atmospheric rotation effects the motion in any given mode is confined to the vertical plane of propagation.

CHAPTER II

AVAILABLE DATA AND DETECTION OF INTERNAL GRAVITY WAVES

2.1. Introduction

Here we shall establish a criterion for the detection of internal gravity waves using Rocket-Grenade Experiment data. Before doing that we give a brief description of the Rocket-Grenade Experiment and consider the accuracy of the data available. This will give an idea as to how reliable are our conclusions. This is important because of the difficulties in the detection of gravity waves.

2.2. Description of the Rocket-Grenade Experiment

The Rocket-Grenade Experiment (RGE) is one of the several techniques employed in the meteorological sounding of the lower atmosphere. The objective of this experiment is to study the phenomena that occur in the upper stratosphere and mesosphere by sampling the structure of these regions. The RGE gives temperature, pressure, density and horizontal wind profiles covering the altitude range of approximately 30 to 90 km.

The experimental technique is based essentially on the reception of sound waves caused by the explosion of sucessive grenades at altitude intervals of a few kilometers launched by a rocket during its ascent. The time and position of each grenade are determined by the DOVAP tracking system by an interference in the CW transmission from the rocket to the ground receiver. A radar is commonly used for background tracking. A

Sound Ranging System having an array of microphones on the ground determines the time of arrival as well as the azimuth and elevation angles of the sound waves from each explosion. A description of the equipment can be found in Friggi (1968) and in more detail in Nordberg and Smith (1964). Measurements of temperature, wind speed, wind direction, pressure, density and humidity up to the height of the first explosion, are obtained by balloons. Using all these data and ray-tracing techniques, average horizontal winds and sound velocity are derived in the layers between successive explosions and from the latter, the temperature. Pressure is extrapolated above the height of balloon measurements using temperature data. The density is obtained using pressure and temperature data.

2.2.1. Data available

The Rocket-Grenade Experiment was initiated in November 1956 but since then the equipment and specially the data reduction and error analysis have undergone considerable modifications. We shall use data from 1960 to 1968 (excluding those of 1965 that were not available) because in the early years the average vertical resolution was much variable. The experiments were conducted at Pt.Barrow (59^{o}N, 156^{o}W), Ft.Churchill (59^{o}N, 94^{o}W), Wallops Island (38^{o}N, 75^{o}W), Natal (6^{o}S, 35^{o}W) and Ascension Island (8^{o}S, 14^{o}W). The data from Ascension is available only up to early 1966 because after that the equipment were transferred to Natal. These places are typical of arctic, sub-arctic, temperate,and tropical locations.

Depending on the geographical location of the stations the observations were divided in three categories: high latitudes (Churchill and

Barrow), medium latitudes (Wallops) and low latitudes (Ascension and Natal). We have analyzed data from a total of 132 firings for which the annual and seasonal distribution in the three categories stated above is given in Table 1 and 2 respectively. Not all data are suitable for the detection of gravity waves because sometimes the vertical resolution is low and sometimes the height range ocvered is too small. The average vertical resolution was approximately 4 km until 1965 and improved to about 3 km after 1966. Depending on the time spacing between the firings at a given place we have divided the observations into two categories that will be referred to as time-spaced experiments (when the period of two sucessive launchings is less than 6 hours) and isolated experiments. We have also some sequences of simultaneous experiments at different places.

2.2.2. Accuracy of the measurements

The errors of the Rocket-Grenade Experiment for measuring meteorological parameters increase with height. The major part of it is due to the inaccuracy in the determination of the time of arrival of sound waves at the microphones. The magnitude of the average error for temperature is about $\pm 4^{o}$ at 70 km and increases steadly to about $\pm 10^{o}$ at 90 km. For wind speed the inaccuracy is much larger and much more variable so that a better way to characterize it is by its percentage values. The magnitude of the average error is about 20% at 70 km and about 40-50% at 90 km. For very strong winds ($\geq$ 80 m/s) it can be as high as 80-90%. The accuracy of the wind direction is a little better, and the error in average is about $\pm$ 15-20^{o}. Although the wind measurements are quite inexact those of wind shears are much better

TABLE I

YEAR / LOCATION	1960	1961	1962	1963	1964	1966	1967	1968
High Latitudes	0	0	2	3	6	19	12	6
Medium Latitudes	1	9	9	4	16	11	7	0
Low Latitudes	0	0	0	0	3	9	13	3

TABLE 2

	WINTER	SPRING	SUMMER	FALL
High Latitudes	26	12	10	0
Medium Latitudes	17	18	12	10
Low Latitudes	10	8	4	5

because the systematic errors cancel out when we take the derivative of the wind with respect to the height. On the average the accuracy of the data from stations at low and medium latitudes (Natal and Wallops) is a little better than that of high latitudes (Churchill and Barrow). After 1967 the accuracy of the measurements at Wallops improved a lot due to the installation of a triple array of microphones. In particular the wind speed measurements there have now an average error less than 15% even at 90 km.

2.3. Detection of internal gravity waves

Although much work has been done on the theory of gravity waves, still more has to be done in its identification and in the determination of some parameters of the wave. With the parameters determined, there would be a better possibility of the identification of the sources. The difficulties are well characterized by the feeling that observations will probably never become sufficiently extensive to completely define tides and gravity waves (Dickinson). Thus it is necessary to use an interplay of theory and observation. This can be done checking, for example, the relations predicted by the theory among the density, pressure, temperature and winds. The search for gravity waves involves the problem of the study of frequency spectra, so the difficulty of identifying gravity waves would be reduced appreciably with a good knowledge of the source because then the search would be restricted to certain parts of the spectrum. But, as quoted before, a knowledge of the sources is lacking.

There are many possible methods for observing gravity waves, which include vapor trails, meteor radar, noctilucent clouds, satellite

measurements, H.F.radars and rocket grenades. In the next section we consider the detection of gravity waves using rocket-grenade observations.

2.3.1. Detection of gravity waves using Rocket-Grenade Experiment Data

All profiles (temperature, pressure, density and winds) given by the Rocket-Grenade Experiment could be used, at least theoretically, for the identification of gravity waves. Two of them are particularly suitable for this; temperature profile and wind profile.Wind profiles have been used by many workers to study atmospheric motions in general and gravity waves in particular (Kochanski, 1964; Revah, 1969). Direct measurements of the temperature can yield valuable information about dynamical processes such as wave motion. In temperature measurements in the E-region made with rocket-borne ion traps, Knudsen and Sharp (1965) observed a temperature profile which strongly suggested the existence of internal gravity waves. Recently some evidence of gravity waves has been found in satellite measurements of ion temperature in the R-egion (Harris et al, 1969) and in incoherent scatter observations (Vasseur and Waldteufel, 1969).

We are going to use only the temperature profiles for the identification of gravity waves because their errors are much smaller than those of the winds. The wind data will be used only as an additional information to investigate some general conditions of the occurence of these waves. As stated before, we have time spaced and isolated data. In some circunstances the detection of wave systems can be done with little ambiguity due to large amplitude of fluctuations on a similar time and spatial

scale so that one can see if the observations are compatible with the theory. The dominant wavelengths can be found from Fourier analysis of the data and time-phase diagrams can indicate if the oscillations are propagating or not. The direction of propagation can be inferred from the time-phase diagram and thus the approximate location of the source can be determined. In practice this is not easy because there are many modes propagating and also there are other superimposed motions. Theoretically the resolution of the question concerning the quasi-steady or dynamical character of the temperature profile could be settled using the density data. Excess temperature and density would be in phase if the temperature variations are produced by adiabatic compression. Excess temperature would occur with a defect of density in a steady state situation. This cannot be done in our case because the density is derived from the temperature data so that they are not independent. Thus the criterion in respect of the time spaced data is that the dominant wavelengths and the period of the wave be in agreement with the theoretical values. Also the relations predicted by the theory must be checked whenever possible. Some information about the location of the source could be obtained using the following method, suggested by Lindzen (1969). If a gravity wave is excited by a local source then its westerly and southerly wind components will be in phase or antiphase. If, on the other hand, the wave is a global standing wave in latitude then the westerly and southerly wind components will be 90^{o} out of phase with each other. These relations can be determined from the theory of gravity waves and tides, but cannot be applied successfully to our data because of the large errors in the measurements of the wind speed and wind direction.

The analysis of isolated data is much more difficult. In some profiles we have either very small oscillations or a single large perturbation and in these cases the analysis becomes subjective. Fig. 5 shows three characteristic temperature profiles. The first profile shows a typical wavy structure; the second shows a wavelike structure which is not as well defined as the first, and the third does not show any perturbation. We infer wavy structures if there are oscillations of at least $10^{o}K$ above 60 km. Only profiles with maximum height above 80 km will be considered in this criterion. The presence of wavy structures in the temperature profile does not necessarily mean that we have waves. This will be discussed in Section 3.3.

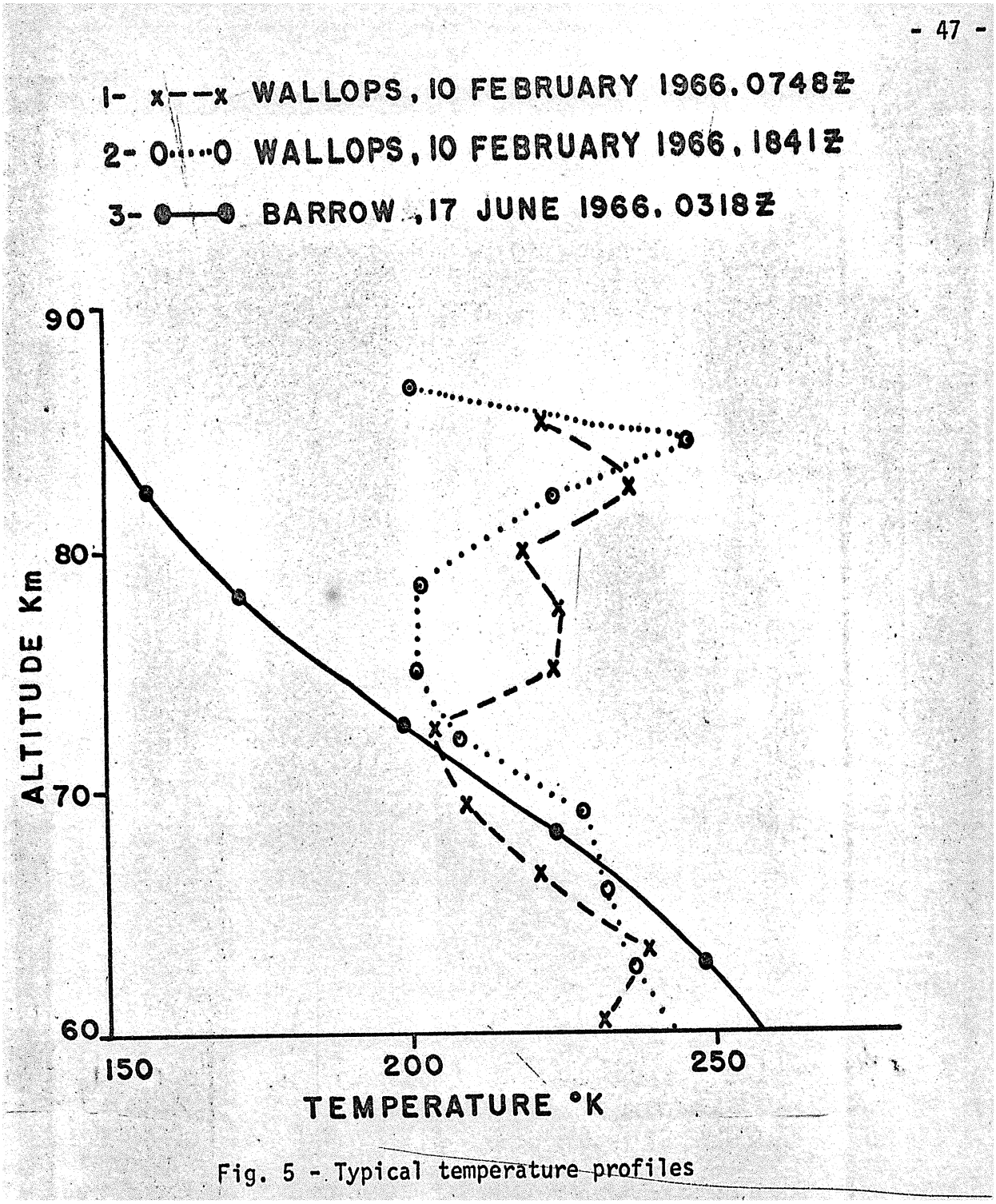

Fig. 5 - Typical temperature profiles

CHAPTER III

DATA ANALYSIS

3.1. Introduction

In this chapter we present the results obtained with the application of the criteria established in Chapter II to the Rocket-Grenade Experiment data. Initially we consider profiles with the best time resolution available (time spaced data) at high, and low latitudes to show evidences of internal gravity waves and to study their properties. (For medium latitudes we do not have sequences of firings with a time resolution good enough for this study). After that we consider the isolated data giving emphasis to the effect of magnetic activity and seasonal variation.

3.2. Time Spaced Data

As previously stated time spaced data are those in which periods between successive firings are no greater than six hours. We shall discuss in detail two sequences of firings at high latitudes because their time resolution is the best available.

3.2.1. Time spaced data at high latitudes

We had rocket grenades firings at high latitudes at Ft. Churchill and Pt.Barrow. In some of the experiments the observed temperature profiles are found to be similar to those detected by Knudsen and Sharp (1965) above 100 km. The wind speed profiles are also similar to those predicted by the theory of gravity waves but these will not be considered in detail because of error considerations.

Two sequences are especially suitable to see evidence of gravity waves, one at Churchill and another at Barrow. On February 1, 1968 four firings were made at Churchill during a period of 135 minutes. The corresponding temperature profiles above 65 km are shown in Fig.6; below this level there are no significant oscillations. The wavelike structure of the profiles is present in all of them. From a comparison of these profiles it is clear that they do not represent a static thermal stratification of the atmosphere; they represent a dynamical behaviour of propagating waves. The third and fourth profiles, which show a temperature fluctuation of about $100^{o}K$ in 45 minutes, are particularly conclusive. The largest temperature excursion is observed in the third profile, where the peak to trough range at 80 km is about $100^{o}K$. The average spacing between crests and troughs is 4-5 km although in some cases it is a high as 11 km. The crests and troughs in the temperature profile could be accounted for by alternate heating and cooling associated with adiabatic compressioms and rarefactions accompanying the waves. From Fig.6 we also see that the temperature fluctuations at the times of the third and fourth firings are almost 180^{o} out of phase and this would suggest a period of about 90 minutes. It would be difficult to explain these waves in terms of tidal waves, having such a low period; also at high latitudes tidal effects are not so significant. According to Lindzen (1969) the time resolution necessary to identify gravity waves of period of 100 minutes is of the order of 20 minutes. Our data have an average time resolution of 45 minutes but even so they do suggest the occurrence of gravity waves.

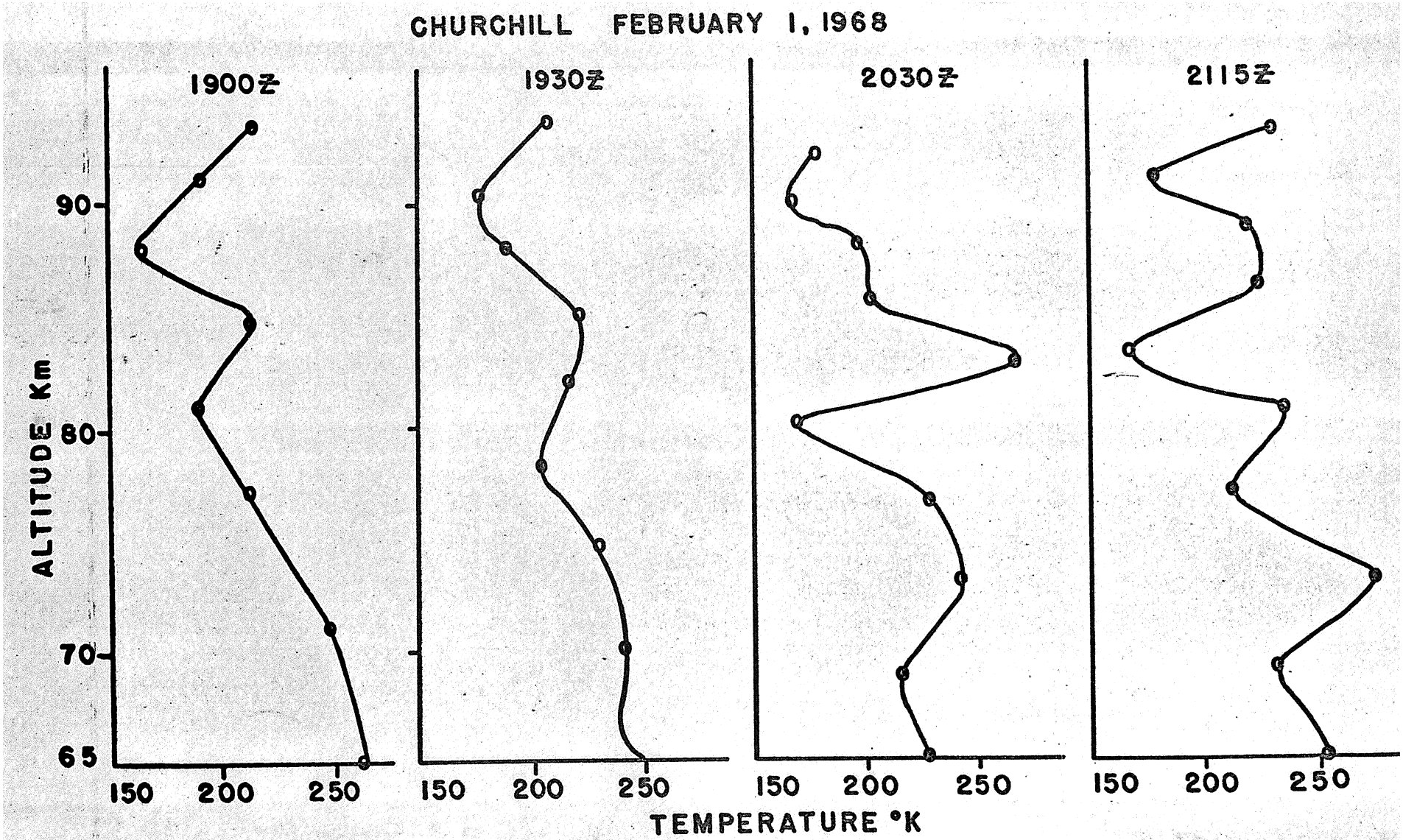
CHURCHILL FEBRUARY 1, 1968
1900Z
1930Z
2030Z
2115Z
ALTITUDE Km
90
80
70
65
150
200
250
TEMPERATURE °K

Fig. 6

The wind profiles above 65 km are shown in Fig.7. We can see immediately the reason why the wind data is not suitable for the study of gravity waves, particularly in the case when there is a strong background wind. The distances between maxima and minima are highly variable but the average value which is about 10 km is in good agreement with the expected one. The values of the wind shears are more precise than the values of the wind speed because in taking the derivative of the wind speed profile some of the systematic errors cancel out. Although the maximum values of the wind speed in the first and third profiles are not precise they show clearly the occurrence of very strong wind shears. The first wind shear is out of phase with the corresponding temperature profile while the second is in phase. The presence of such large vlaues of wind shears suggest that they play an important role in the generation of these waves. The values of the wind shears in the first and third profiles are about 70 m/sec km^{-1} which, although very large, is not unlikely. Kochanski (1964) has reported a maximum value of wind shear of 120 m/sec km^{-1} at 105 km at Wallops.

Let us now see how far the observed features are consistent with the idea of internal gravity waves. For atmospheric gravity waves the dominant wavelength for a realistic case (under the hypothesis stated in section 3.4.2) is about 12 km up to an altitude of 100 km and increases above this height (Midgley and Liemohn, 1966) and the period of the wave is about 200 minutes. The phase fronts propagate downwards while the energy travels almost horizontally with a slightly upward component. The dominant wavelength given by the temperature profile is about 9 km. A typical example

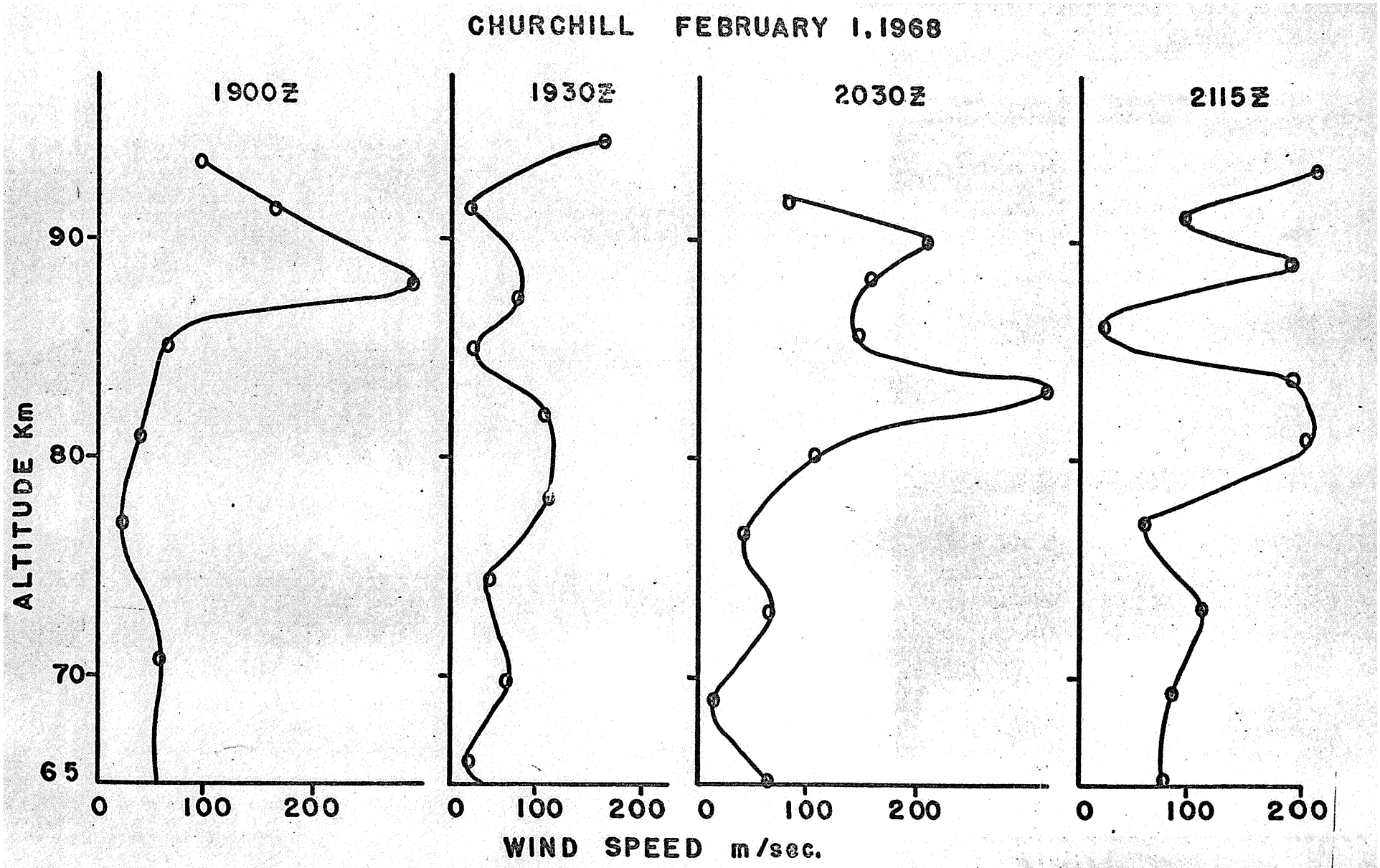
CHURCHILL FEBRUARY 1, 1968
1900Z
1930Z
2030Z
2115Z
ALTITUDE Km
90
80
70
65
0
100
200
WIND SPEED m/sec.

Fig. 7

of harmonic analysis of one of the temperature profiles is shown in Fig.8. The spectral analysis was done taking 16 samples of temperature profile from above to below with 1.33 km between sucessive points and taking the Fourier transforms of the sampling. In some cases the analysis was done also with 32 samples for a larger height range. As could be predicted, the figure presents a broad maximum around 10 km showing that we do not have only one dominant but several modes. The broad maximum also shifts a little from one profile to another of the same sequence.

The time-phase diagram for the 9 km wavelength is given in Fig. 9 for the upgoing and downcoming phase propagation. The upgoing phase propagation gives a period of 45 minutes while the downcoming phase propagation gives a period of the order of 90 minutes. The choice between the two values and of the direction of propagation must be made using consideration of energy dissipation and compatibility with the periods of other wavelengths close to the dominant one. Since the energy dissipation would be excessive for the second case and it would be difficult to identify a powerful source above 100 km which would generate such waves independently of magnetic activity, we conclude that the downward phase propagation is more probable. Both problems, i.e. the determination of the dominant wavelength and of the direction of propagation, are made more difficult by the presence of several propagating waves and of reflections at various levels.

Another check on the agreement between theory and the behaviour of the profiles can be made by calculating the amplitude of the temperature fluctuation. Until dissipation becomes severe in any given mode, that particular

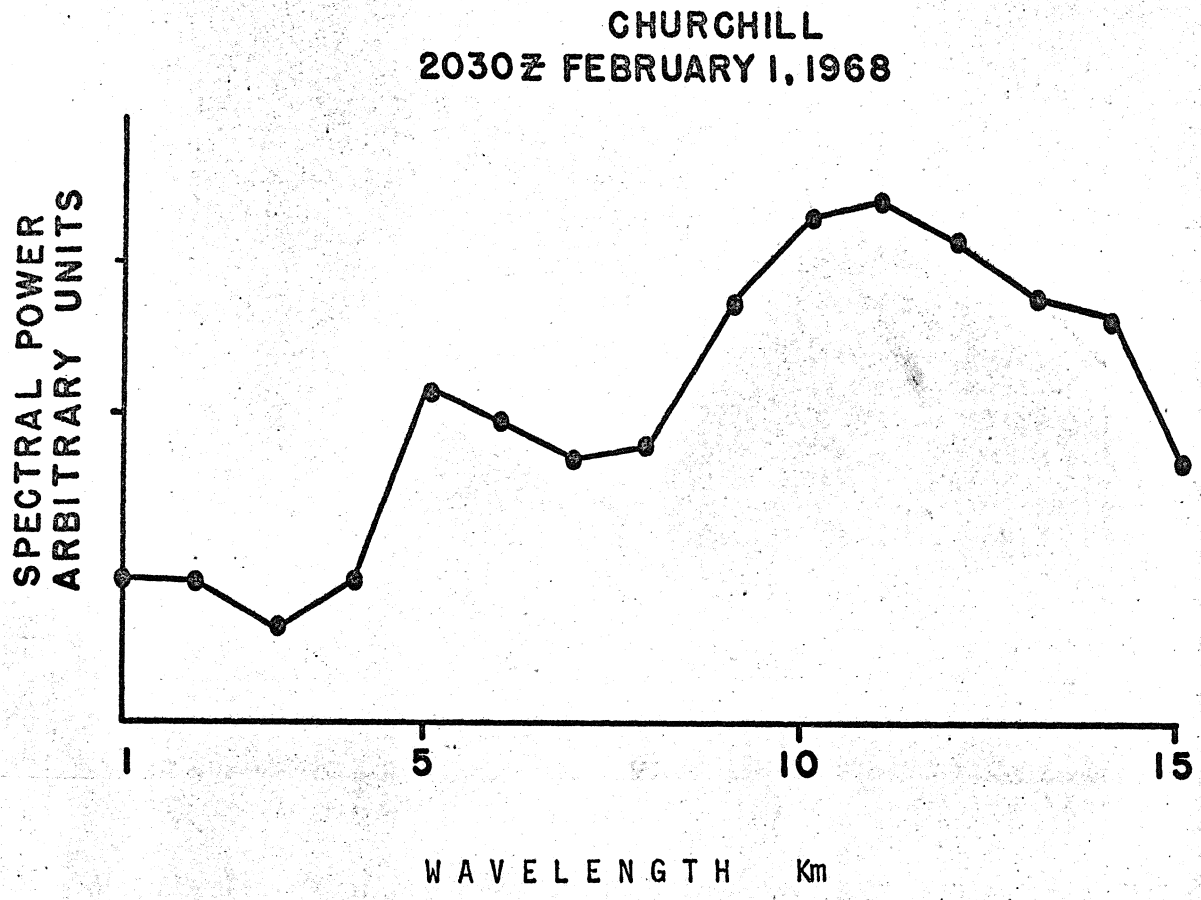

Fig. 8 - Typical Fourier spectrum of a temperature profile

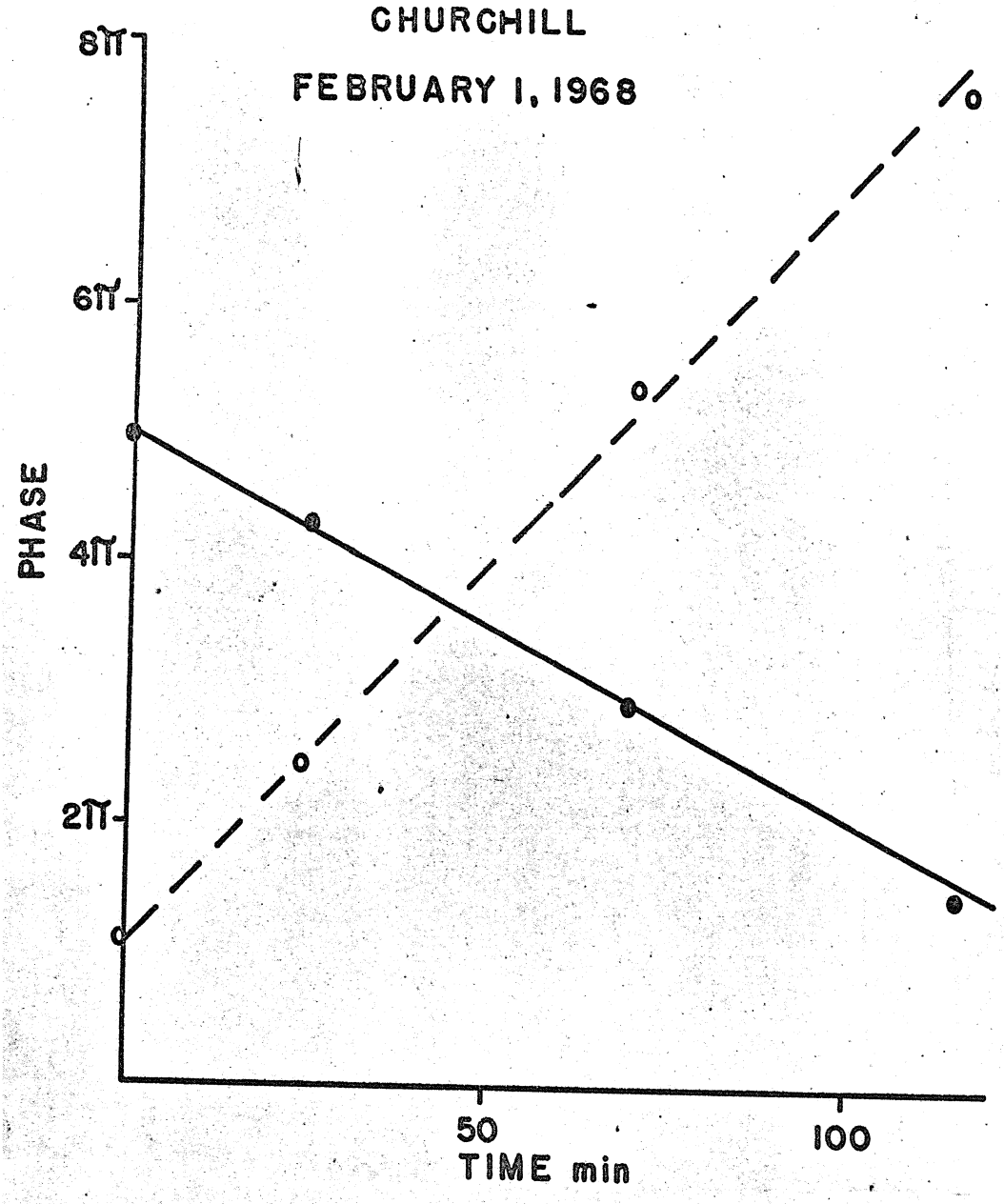

Fig.9 - Phase-time diagram for the dominant component (9 km)

propagating mode produces adiabatic heating and cooling during its oscillation for which the amplitude is given by (Hines, 1965)

$$\frac{\delta T}{T} = (P - R)\frac{V'_x}{C} \tag{3.1}$$

where P, R are given in (1.26) - (1.28) and V'_x is the fluctuation component of the horizontal wind speed. If λ_z is not much greater than the local scale height and the period of the wave is much greater than the Brunt-Vaisala period (3.1) can be written as

$$\frac{\delta T}{T} \simeq \pm i(\gamma - 1)\frac{V'_x}{C} \tag{3.2}$$

here i indicates a phase quadrature between the time or phase of maximum in δT and V'_x while the plus or minus uncertainty is related to the uncertainly in the direction of phase propagation relative to the direction of V'_x. In our case the dominant component does not exceed appreciably the local scale height (for the mesosphere H = 6 km). Taking $T \sim 200^{o}K$, $C \sim 280$ m/sec and $V'_x \sim 50$ m/sec, we have $\delta T \sim 25^{o}K$. This estimate agrees with the observations on the average; however, it provides only a check on the order of magnitude of the fluctuations, since in the actual observations we may not be dealing with a single wave and the value of the wind speed is not only inaccurate but also highly variable.

Let us now determine the energy loss with height. The energy density is given by $\rho V'^{2}_x/2$ and the vertical energy flux by

$$F_z = \rho V'^2_x \frac{V_z}{2} \tag{3.3}$$

where V_z is the vertical component of the group velocity given by $\partial\omega/\partial k_z$ (section 1.6.1). The decrease of energy flux with height is given by $-\frac{dF_z}{dz}$. Kochanski (1964) found that for the 70 - 140 km height range

$$\rho V'^2_x \alpha \exp -(z/H) \tag{3.4}$$

Using (3.3) and (3.4) and considering that the vertical variation of V_z is negligible compared with the variation of the mean energy density, the rate of energy loss becomes

$$\varepsilon = V'^2_x \frac{V_z}{2H} \tag{3.5}$$

The vertical group velocity for periods much larger than the Brunt-Vaisala period (about 5 minutes in the mesosphere) is given by

$$V_z \simeq \frac{\lambda_z}{\tau} \tag{3.6}$$

Using (3.5), (3.6) and the values of the present set of observations we obtain $\varepsilon \simeq 0{,}35$ watt/kg which corresponds to a heating rate of the order of 30^{o}C/day. This value is rather high but even so it gives an idea of the order of magnitude of the heating rate.

Another set of launches with a good time resoltuion at high latitudes is from Pt. Barrow for January 31 - February 1, 1967. During this

period five rockets were launched within ten hours. The corresponding temperature and wind speed profiles are shown in Fig. 10. The temperature fluctuations present highly variable amplitudes; in this case also we have strong background winds but not as strong wind shears. The profiles suggest an oscillating characteristic but their average amplitudes are smaller than in the previous case. The distance of the successive peaks and throughs of the temperature profiles is represented in Fig. 11. The average value for each 10 km interval is also indicated. In spite of the high variability of the half-wavelength (as called by Kochanski) the average value which is of the order of 9 km gives a surprisingly good agreement with the expected value. The spectral analysis agrees with this value but there is a larger variability of the dominant component from one profile to another. The period of the wave associated with the dominant component as deduced by the corresponding time-phase diagram is of the order of 180 minutes but it might also be 90 minutes. Our time resolution does not allow to resolve this indetermination. Smaller values of the period (for example 45 minutes) may also be possible but are unlikely and incompatible with theoretical considerations as in the previous case. All these factors suggest that the observations really represent gravity waves since it would be difficult to explain them in terms of other motions; the tides, for example, are practically negligible at such high latitudes.

The first sequence of launches was made during a period in which the K_p index was 2 and the daily K_p was 18. During the second sequence the K_p indices were 1-, 2, ,+, 2-, and the period was magnetically very quiet

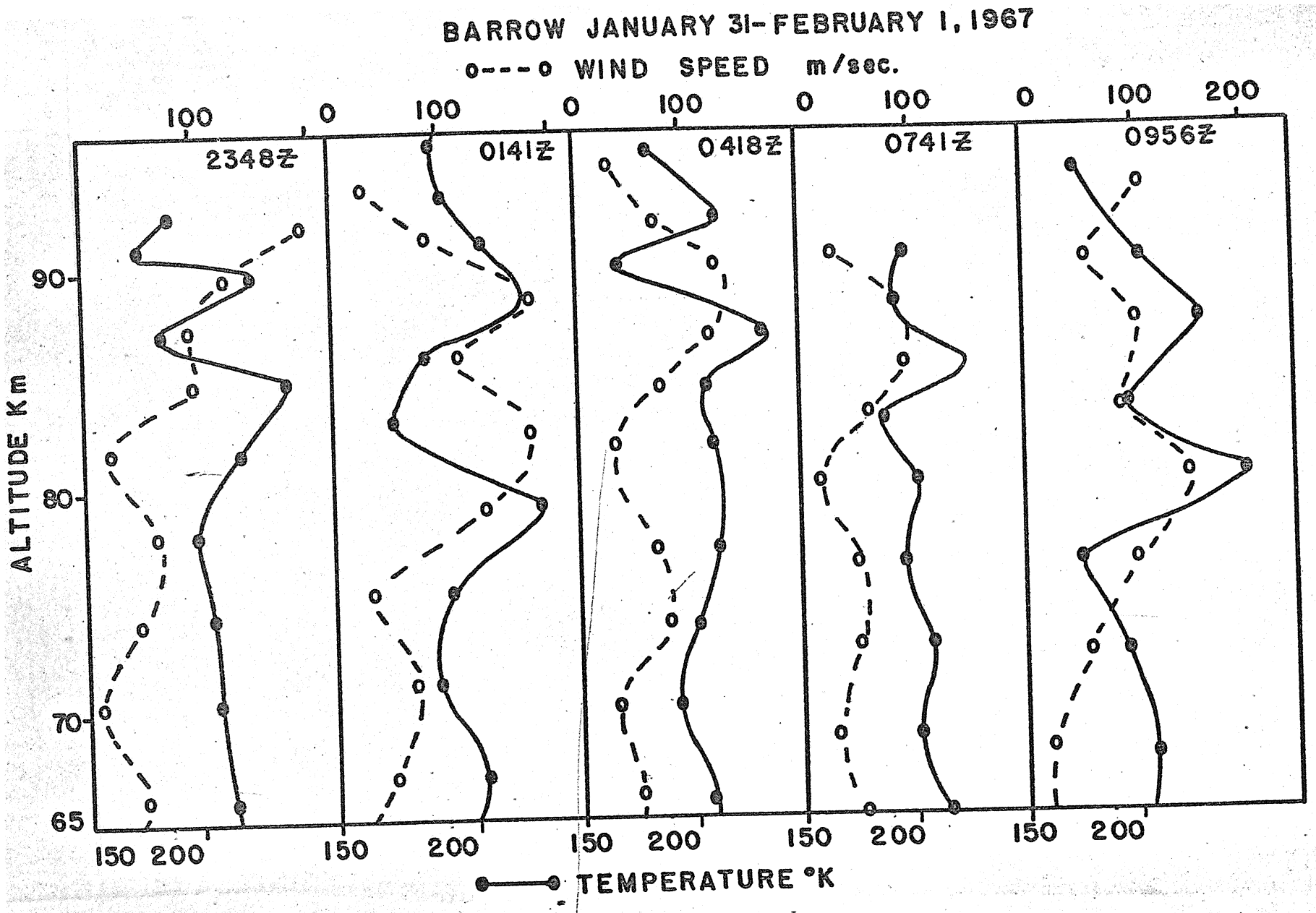
BARROW JANUARY 31-FEBRUARY 1, 1967
o---o WIND SPEED m/sec.
100 0 100 0 100 0 100 0 100 200
2348Z
0141Z
0418Z
0741Z
0956Z
ALTITUDE Km
90
80
70
65
150 200
TEMPERATURE °K

Fig. 10

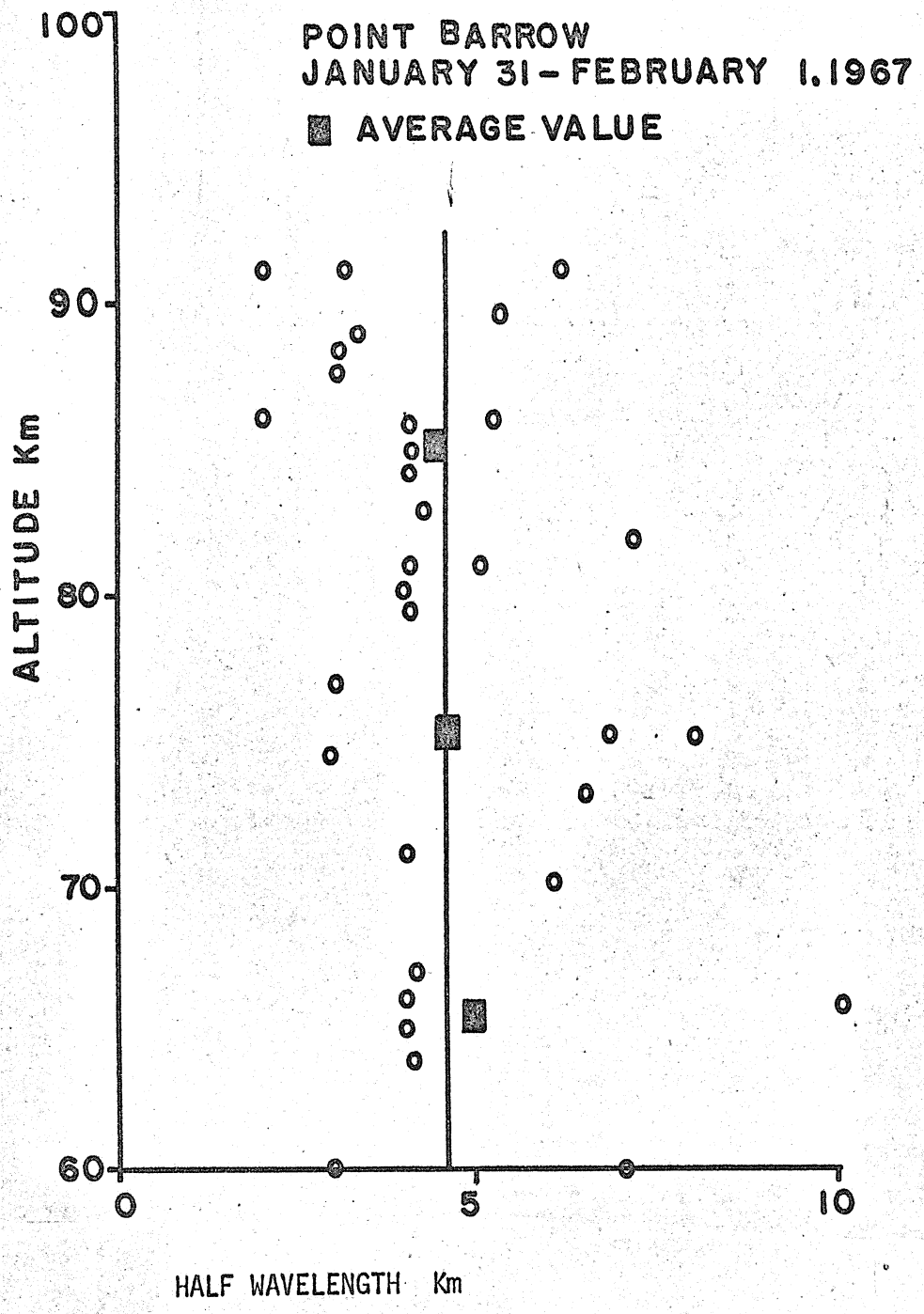

Fig. 11 - Distance between maxima and minima of temperature profiles

(the daily K_p were 4 and 9- respectively). This suggests that the main mechanism for the generation of these waves must not have a large correspondence with magnetic activity. An interesting feature of both sets of profiles is the strong horizontal wind speeds and, in the first case, very strong wind shears. The relation between the possibility of the occurrence of waves and magnetic activity will be discussed in more detail in section 3.3 for various latitudes. If better wind measurements were available, the test referred to in section 2.4 could be applied to verify whether the source of these waves is local or not.

3.2.2. Time spaced data at low latitudes

The temperature and wind speed profiles corresponding to four rocket fired on October 1-2, 1966 at Natal are shown in Fig.12. It is evident from a comparison of these profiles that the idea of a quasi-steady state of the atmosphere is ruled out. Furthermore, as discussed by Knudsen and Sharp (1965), such a quasi steady state where conduction would be the dominant heat transfer mechanism, would not persist during night hours when some of these profiles have been observed. The largest temperature oscillation is observed in the second firing, where the peak to trough range is about $100^{o}K$. The almost constant spacing between temperature maxima and minima gives a wavelength of about 10-12 km and a comparison of sucessive profiles suggests a downward phase progression. The experimental temperature profiles are in agreement with those expected, once we accept that under such conditions the level of the mesopause would undergo fluctuations and hence, it would be difficult to determine a characteristic mesopause height.

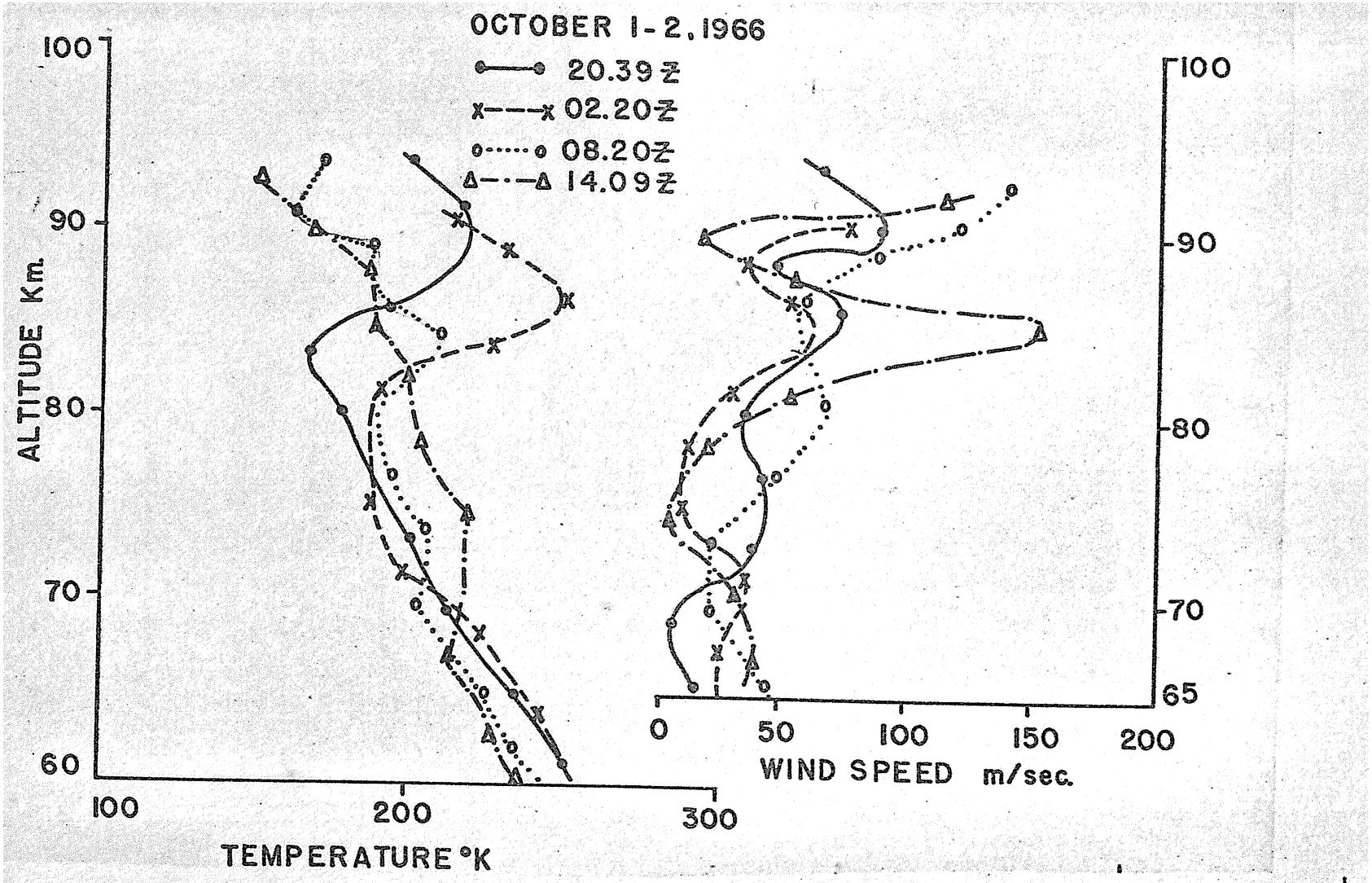

Fig. 12 - Temperature and wind speed profiles at Natal

The wave character of the profiles could be associated with either tidal waves or internal gravity waves. The temporal resolution required for choosing between the two type of waves is much greater than that provided by the present observations. The amplitude of temperature variation given by (3.1) gives the same order of magnitude as that of Churchill which agrees with the present observations. The period determined by the time-phase diagram was about 300 minutes, but it could also be 150 minutes. The period during which the launches were made was magnetically very quiet; the maximum K has 1+ and the daily K_p were 11 and 5- respectively.

3.3. Analysis of isolated data

As previously stated, the analysis of isolated data for detection of waves, and especially of gravity waves is not only difficult but also doubtful and somewhat subjective. So we must be extremely careful in deriving conclusions from isolated profiles; otherwise meaningless correlations will result. Remembering this we consider a temperature profile to have a wavelike structure whenever it presents oscillations of at least $10^{o}K$ above 60 km. A perturbation in the temperature profile does not necessarily represent a wave; it might represent simply a local heating or cooling. If it really represents a wave this can be propagating wave or an evanescent one. Finally the propagating waves can be tidal waves, planetary waves, or internal gravity waves. When we have a propagating wave we can assume that it represents a gravity wave if it has a small wavelength ($\leq$ 12 km).

With our isolated data we attempt to analyze general effects such as seasonal distribution of wavy profiles, the influence of magnetic activity

and strong winds and wind shears. The influence of strong background winds and wind shears is not clear from our data due to the inaccuracy of wind measurements. The effect of magnetic activity was studied using the daily K_p index and dates of magnetic storms whenever available. Using Thomson scatter at St.Santin (45^oN), Testud and Vasseur (1969), have observed a good correlation between strong magnetic activity, which they characterized by a daily $K_p > 16$, and inferred the presence of gravity waves in the thermosphere. We shall see if the same happens at lower altitudes and in various seasons.

The effect of magnetic activity and seasonal distribution of wavy profiles for medium latitudes is characterized by the data of Table 3. The more doubtful cases were not considered; clear wavy or non-wavy temperature profiles in fall are lacking

TABLE 3

	OSCILLATIONS		NO OSCILLATIONS	
	$\Sigma K_p \geq 16$	$\Sigma K_p < 16$	$\Sigma K_p \geq 16$	$\Sigma K_p < 16$
Spring	1	3	5	0
Winter	3	5	0	2
Summer	1	0	3	4

From this table we can see immediately that we do not have a definite behaviour related to the magnetic activity throughout the year. The proabability of the occurrence of wavy profiles seems to be large in winter independently of the magnetic activity. For summer this probability seems to

be very low, which agrees with the lack of occurrence of other waves such as planetary waves, although the reasons may be different. For spring we cannot conclude anything, but it may represent a transition between winter and summer conditions.

Table 4 show the relation between magnetic activity and seasonal distributions of wavy profiles at high latitudes. Here also the

TABLE 4

	OSCILLATIONS		NO OSCILLATIONS	
	$\Sigma K_p \geq 16$	$\Sigma K_p < 16$	$\Sigma K_p \geq 16$	$\Sigma K_p < 16$
Fall	0	0	0	1
Summer	0	0	4	6
Winter	3	3	2	1
Spring	1	1	3	4

probability of wavy profiles is maximum in winter and minimum in summer and it seems that the magnetic activity does not play an important role in the appearance of waves at least at lower altitudes. For low latitudes the results are shown in Table 5 and the conclusions are similar to those of the previous cases although the inadequate amount of data prevents a definite statement

TABLE 5

	OSCILLATIONS		NO OSCILLATIONS	
	$\Sigma K_p \geq 16$	$\Sigma K_p < 16$	$\Sigma K_p \geq 16$	$\Sigma K_p < 16$
Fall	1	0	0	0
Summer	0	0	2	0
Winter	1	3	0	1
Spring	2	0	0	0

During periods of high magnetic activity there is a general shift of the temperature profiles to larger values, especially at high latitudes; also the occurrence of strong wind shears at about 85 - 90 km is common at such occasions. One puzzling problem is the fact that sometimes we have strongly wavelike wind speed profile although there is no appreciable fluctuation in the temperature profile and vice-versa. The first case might signify evanescent waves and the second no waves at all but local heating or cooling due to other effects; this can be clarified only with wind measurements of much better accuracy than ours.

CHAPTER IV

GENERATION OF TURBULENCE BY GRAVITY WAVES

4.1. Introduction

In this chapter we present a brief discussion of the generation of turbulence in the upper atmosphere by internal atmospheric gravity waves. Initially we consider some mechanisms that can generate turbulence in the atmosphere, giving more attention to the generation of instabilities caused by gravity waves, which can produce turbulence in quiescent regions of the atmosphere. After that we consider the probability of the production of these instabilities using some of the conclusions of chapter III.

4.2. Generation of turbulence

The quantity used as a criterion for the development of turbulent motion is the Richardson number

$$R_i = \frac{\omega_B^2}{\left|\frac{\partial V_x}{\partial z}\right|^2}$$

where ω_B is the Brunt-Vaisala frequency given by

$$\omega_B^2 = - g \left| \frac{1}{\rho} \frac{\partial \rho}{\partial z} + \frac{g}{\gamma R T} \right|$$

When the Richardson number is less than unity the creation of turbulence exceeds its rate of dissipation. In a nonturbulent region turbulence can be created if the Richardson's number is greater than a critical value

$R_i \cong 0.08$ (Hodges, 1967). The wind shear required for the production of turbulence in a nonturbulent atmosphere at about 100 km is of the order of 80 m/sec km^{-1}. The probability of the occurrence of such large wind shears is extremely low. In our case with a height resolution of about 3 km, the variation between two successive points would have to be about 200 m/sec, which practically never happens. So it is unlikely that at these heights turbulence can be produced by wind shears.

Hodges (1967) has shown that gravity waves can sustain turbulence generating instabilities by the variation of pressure density and temperature and so by the change of ω_B. Instabilities are generated when the Richardson number is negative, which corresonds to a superadiabatic condition. The instabilities must extract energy from the wave transporting heat vertically in an attempt to destroy the local superadiabatic lapse rate, thus resulting in viscous damping of the wave. He has found that gravity waves have sufficient amplitudes to produce regions in which convective instabilities may occur at least 25% of the time.

Since the errors of the wind speed measurements are very large we are not able to determine the percentage time when the amplitude is enough to produce convective instabilities, capable of producing turbulence. We can see by inspection that in the case of the two sets discussed in chapter III there must have been conditions for generation of turbulence. Using the values of the vertical wavelength and period of the first set, from Hodges model we get an eddy diffusion coefficient of the order of 2×10^6 cm^2/sec which may be reasonable during winter.

The general nature of the profiles shows that the frequency of occurrence of strong winds in winter is larger than in other seasons at all latitudes and so is the occurrence of wavelike profiles. Thus during winter months the generation of turbulence must be more frequent than during nonwinter months. We also conclude that the analysis of wind speed profiles above may not be very reliable to determine turbulence because from isolated profiles it is not possible to determine whether the waves are propagating or not.

CHAPTER V

CONCLUSIONS

From the analysis and discussion presented in the previous chapters we can derive the following conclusions.

Gravity waves can be detected with a good degree of certainty using Rocket-Grenade Experiment data whenever the time resolution is better than about a half period. In such cases the consistency of the theoretical relations can be checked and the agreement between the theoretical predictions and observations is quite good. If good wind measurements are available, it would be possible to test the theory more completely and to make some conclusions about the sources. The best way to detect gravity waves seems to consider both temperature and wind profiles (when the latter has reasonable accuracy).

The magnetic activity does not seem to play as important role in the appearance of gravity waves as one would have expected on the basis of the studies reported in the literature for higher altitudes; its main effect seems to be a general shift of the temperature profile towards greater values which is consistent with the general heating of the atmosphere during magnetic storms. The probability of the occurrence of wavy profiles in general, and of gravity waves in particular, is maximum in winter and minimum in nonwinter months at all latitudes; this effect is more pronounced at high latitudes. In this respect the occurrence of gravity waves during very quiet

magnetic conditions is very significant. The relation between strong winds and wind shears during winter month suggests a higher probability of occurrence of turbulence during winter months.

ACKNOWLEDGMENTS

I am greatly indebted to Dr.D.B.Rai for his constant help and interest, to Dr.B.R.Clemesha, Dr.L.Gylvan Meira and Dr.S.K.Alurkar for valuable suggestions. I am also indebted to Dr.Fernando de Mendonça whose interest made this work possible. Thanks are also due to all friends in CNAE for providing incentive and to Miss Sandra Cristina Porto for typing this thesis.

REFERENCES

Chimonas, G., The equatorial electrojet as a source of long period travelling ionospheric disturbances, Planet.Space Sci.18, 583-589, 1970.

Chimonas G. and Hines, C.O., Atmospheric gravity waves launched by auroral currents, Planet.Space Sci.18, 565-582, 1970a.

Chimonas G. and Hines, C.O., Atmospheric waves induced by a solar eclipse, J.Geophys.Res.75, 875, 1970b.

Chrzanowski, P.G., Greene, K.T.Lemmon and J.M.Young, Traveling pressure waves associated with geomagnetic activity, J.Geophys.Res.66, 3727-3723,1961.

Cole, K.D., A source of energy for ionosphere, Nature, 194, 75, 1962a.

Cole, K.D., Atmospheric blow-up at the auroral zone, Nature, 194, 761, 1962b.

Davies, K., D.M.Baker, N.J.F.Chang, Comparison between formulas for ionospheric radio propagation and atmospheric wave propagation, Radio Sci.,4, 231-234, 1969.

Friedman, J.P., Propagation of internal gravity waves in a thermally stratified atmosphere, J.Geophys.Res.71, 1033-1054, 1966.

Friggi, S.R., The determination of upper atmosphere metereological parameters by means of the Rocket-Grenade Experiment, Thechnical Report LAFE-71, Comissão Nacional de Atividades Espaciais, S.J.Campos-SP-Brasil, 1968.

Gossard, E.E., Vertical flux of energy into the lower ionosphere from internal gravity waves generated in the troposphere, J.Geophys.Res.67, 745-757, 1962.

Harris, K.K., G.W.Sharp and W.C.Knudsen, Gravity waves observed by ionospheric temperature measurements in the F-region, J.Geophys.Res.74, 197-204, 1969.

Hines, C.O., Internal atmospheric gravity waves at ionospheric heights, Can. J.Phys., 38, 1441-1481, 1960.

Hines, C.O., Minimum Vertical scale sizes in the wind structure above 100 kilometers, J.Geophys.Res.64, 2847-2848, 1964.

Hines, C.O., Atmospheric gravity waves: a new toy for the wave theorist, Radio Sci. 69D, 375-380, 1965a.

Hines, C.O., Heating of the upper atmosphere, J.Geophys.Res.70, 177-184, 1965b.

Hines, C.O., On the nature of traveling ionospheric disturbances launched by low altitude nuclear explosion, J.Geophys.Res., 72, 1877-1882, 1967.

Hines, C.O., Notes of the course on internal gravity and acoustic waves in planetary and solar atmospheres held at Boulder, Junes 17 - July 19, 1968.

Hodges, R.R., Jr., Vertical transport of minor constituents in the lower thermosphere by nonlinear processes of gravity waves. Univ.of Texas at Dallas, February 1970.

Hodges, R.R.,Jr., Generation of turbulence in the upper atmosphere by internal gravity waves, J.Geophys.Res.72, 3455-3458, 1967.

Hodges, R.R.,Jr., Eddy diffusion coefficients due to instabil ities in internal gravity waves, J.Geophys.Res.74,4087-4090, 1969.

Hooke, W.H., Ionospheric irregularities produced by internal atmospheric gravity waves, J.Atmospheric Terrest.Phys.30, 795-824, 1968.

Hunsucker R.D. and L.H.Tveten, Large traveling disturbances observed at midlatitudes utilizing h.f. backscatter techniques, J.Atmospheric Terrest.Phys.29, 909-916, 1967.

Knudsen, W.C., and G.W.Sharp, Evidence for temperature stratification in the E-region, J.Geophys.Res.70, 143-160, 1965.

Kochanski, A., Atmospheric motions from sodium cloud drifts, J.Geophys.Res., 69, 3651-3662, 1964.

Lindzen, R., Data necessary for the detection and description of tides and gravity waves in the upper atmosphere, J.Atmospheric Terrest.Phys. 31, 449-456, 1969.

Lomax, J.B., Nielson D.L., Observation of acoustic gravity wave effect showing geomagnetic field dependence. J.Atmospheric Terrest.30, 1033-1050, 1968.

Maeda, K., and T.Watanabe, Infrasonic waves from the auroral zone, NASA-TN-D-2138, Junes, 1964.

Midgley, J.E. and H.B.Leimohn, Gravity waves in a realistic atmosphere, J. Geophys.Res.,71, 3729-2748, 1966.

Nordberg, W. and Smith, W.S., The Rocket-Grenade Experiment. NASA. Technical Note D-2107, March 1964.

Pitteway, M.L. and C.O.Hines, The reflection and ducting of atmospheric acoustic gravity waves, Can.J.Phys.41, 1935-1948, 1963.

Press, F., and D.Harkrider, Propagation of acoustic-gravity waves in the atmosphere, J.Geophys.Res.,67, 3889-3908, 1962.

Revah, I., Étude des vents de petite échelle observés au moyen des traineés météoriques, Ann Géophys.25, 1-45, 1969.

Row, R.V., Acoustic-gravity waves in the upper atmosphere due to a nuclear detonation and an earthquake, J.Geophys.Res.72, 1599-1610, 1967.

Testud, J. and G.Vasseur, Ondes de gravité dans la thermosphere, Ann Géophys. 25, 525-546, 1969.

Testud, J. and G.Vasseur, Gravity waves generated during magnetic substorms. Paper presented at International Symposium on waves in the upper atmosphere (Toronto, 19-22 January, 1970).

Thome, G., Long period waves generated in the polar ionosphere during the onset of magnetic storms, J.Geophys.Res.73, 6319-6336, 1968.

Tolstoy, I., The theory of waves in stratified fluids including the effects of gravity and rotation, Rev.Mod.Phys.35, 207-230, 1963.

Tveten, L.H., Ionospheric mitons observed with high frequency backscatter sounders, J.Res.NBS, 65D, 115, 1961.

Vasseur, G. and P.Waldteufel, Thomson scatter observations of a gravity wave in the ionospheric F-region, J.Atmospheric Terrest.Phys.31, 885-888, 1969.

Wilson, C.R. and S.Nichparenko, Infrasonic waves and auroral activity, Nature, 214, 1299, 1967.